



1 **Source apportionment of ambient particle number concentrations in central Los**  
2 **Angeles using positive matrix factorization (PMF)**

3

4 M.H. Sowlat<sup>1</sup>, S. Hasheminassab<sup>1</sup>, C. Sioutas<sup>1</sup>

5

6

7 <sup>1</sup>University of Southern California, Department of Civil and Environmental Engineering

8 \*Corresponding author

9 3620 S. Vermont Ave. KAP210, Los Angeles, CA 90089

10 E-mail: sioutas@usc.edu

11 Telephone: 213-740-6134

12 Fax: 213-744-1426

13

14

15

16 **Abstract**

17 In this study, the Positive Matrix Factorization (PMF) receptor model (version 5.0)  
18 was used to identify and quantify major sources contributing to particulate matter (PM)  
19 number concentrations, using PM number size distributions in the range of 13 nm to 10 µm  
20 combined with several auxiliary variables, including black carbon (BC), elemental and  
21 organic carbon (EC/OC), PM mass concentrations, gaseous pollutants, meteorological, and  
22 traffic counts data, collected for about 9 months between August 2014 and 2015 in central  
23 Los Angeles, CA. Several parameters, including particle number and volume size distribution  
24 profiles, profiles of auxiliary variables, contributions of different factors in different seasons  
25 to the total number concentrations, diurnal variations of each of the resolved factors in the  
26 cold and warm phases, weekday/weekend analysis for each of the resolved factors, and  
27 correlation between auxiliary variables and the relative contribution of each of the resolved  
28 factors, were used to identify PM sources. A six-factor solution was identified as the  
29 optimum for the aforementioned input data. The resolved factors comprised nucleation,  
30 traffic 1, traffic 2 (having a larger mode diameter than traffic 1 factor), urban background  
31 aerosol, secondary aerosol, and soil/road dust. Traffic sources (1 and 2) were the major  
32 contributor to PM number concentrations, collectively making up to above 60% (60.8-68.4%)  
33 of the total number concentrations during the study period. Their contribution was also  
34 significantly higher in the cold phase compared to the warm phase. Nucleation was another  
35 major factor significantly contributing to the total number concentrations (an overall



1 contribution of 17%, ranging from 11.7% to 24%), having a larger contribution during the  
2 warm phase than in the cold phase. The other identified factors were urban background  
3 aerosol, secondary aerosol, and soil/road dust, with relative contributions of approximately  
4 12% (7.4-17.1), 2.1% (1.5-2.5%), and 1.1% (0.2-6.3%), respectively, overall accounting for  
5 about 15% (15.2-19.8%) of PM number concentrations. As expected, PM number  
6 concentrations were dominated by factors with smaller mode diameters, such as traffic and  
7 nucleation. On the other hand, PM volume and mass concentrations in the study area were  
8 mostly affected by sources having larger mode diameters, including secondary aerosols and  
9 soil/road dust. Results from the present study can be used as input parameters in future  
10 epidemiological studies to link PM sources to adverse health effects as well as by policy  
11 makers to set targeted and more protective emission standards for PM.

12

### 13 **1. Introduction**

14 Numerous epidemiological studies have provided compelling evidence linking exposure  
15 to ambient particulate matter (PM) with increased risk of respiratory and cardiovascular  
16 diseases, hospitalization, and premature mortality (Brunekreef and Forsberg, 2005; Dockery  
17 and Stone, 2007; Miller et al., 2007; Pope et al., 2004; Pope Iii et al., 2002; Gauderman et al.,  
18 2015). According to the most recent global burden of disease study, over 3 million premature  
19 deaths annually occur all around the globe due to exposure to ambient PM (Lim et al., 2013).  
20 It should, however, be noted that most of these epidemiological studies have related the  
21 aforementioned health outcomes with solely the mass concentrations of PM and, therefore, do  
22 not adequately represent submicron particles (Ogulei et al., 2007), mainly because this PM  
23 fraction contributes negligibly to total ambient PM mass (Delfino et al., 2005; Vu et al.,  
24 2015). More recently, studies have associated human health effects with particles  
25 characteristics other than mass concentration, including size, number concentration, chemical  
26 composition, and even surface area (Brook et al., 2010; Kasumba et al., 2009; Lighty et al.,  
27 2000; Chen et al., 1991; Dreher et al., 1997; Oberdörster et al., 1994; Peters et al., 1997; Delfino  
28 et al., 2010; Davis et al., 2013). Even though our knowledge of which particle characteristic  
29 (mass, size, surface area, etc.) can be considered as the best predictor for human health  
30 outcomes is limited, there is growing evidence highlighting the critical role of particle size  
31 and number concentrations from a human health effect perspective (Vu et al., 2015). For  
32 example, studies have indicated that ultrafine particles (UFP, i.e. particles with an  
33 aerodynamic diameter of <100 nm) have higher toxicity per unit mass (Donaldson et al.,  
34 1998; Li et al., 2003; Nel et al., 2006; Oberdörster et al., 2002), have higher deposition



1 efficiencies in the lung (Venkataraman, 1999), and penetrate deeper into the alveolar regions  
2 of lungs (Sioutas et al., 2005). Additionally, several studies have also found that PM number  
3 concentrations (mostly UFPs) can be associated with adverse effects on human health,  
4 particularly for cardiovascular diseases (Delfino et al., 2005;Peters et al., 1997;Wichmann et  
5 al., 2000).

6 As a consequence, regulations on PM number concentrations have already been  
7 implemented on motor vehicle emissions in few countries. For instance, the Euro 5b and 6  
8 have set a limit to particle number emission factors, in addition to particle mass emission  
9 limits, for heavy-duty and gasoline vehicles (<http://www.dieselnet.com/standards/eu/ld.php>,  
10 accessed 20 October 2015). It is also expected that this approach be gradually adopted in  
11 other parts of the world (Friend et al., 2013), based mainly on the critical health implications  
12 of the PM number concentrations, especially in smaller fractions like UFP. This emphasizes  
13 the necessity of identification and quantification of PM sources based on number as well as  
14 mass (Friend et al., 2013). This allows for source-specific assessment of health effects of  
15 exposure to PM to provide us with the knowledge required to develop efficient control  
16 strategies for PM emissions from major sources to minimize those health effects (Yue et al.,  
17 2008).

18 Positive Matrix Factorization (PMF) is one of the most widely used receptor models  
19 that have been successfully applied to identify and quantify sources of atmospheric particles.  
20 The vast majority of previous efforts has been devoted to the identification of sources that  
21 contribute to the mass of particles using PMF on chemically-speciated PM mass data in  
22 different parts of the world (Sowlat et al., 2013;Sowlat et al., 2012;Dutton et al., 2010;Lim et  
23 al., 2010;Alleman et al., 2010;Sofowote et al., 2015). Recently, attempts have been made to  
24 characterize sources that contribute to particle number, rather than mass, using PMF applied  
25 to particle number size distribution data. These studies have adopted different approaches in  
26 their source apportionment, including: (1) using particle number size distribution together  
27 with gaseous pollutants, chemical composition, meteorological, or traffic data in the PMF  
28 analysis (Beddows et al., 2015;Harrison et al., 2011;Kasumba et al., 2009;Ogulei et al.,  
29 2007;Ogulei et al., 2006b;Thimmaiah et al., 2009;Zhou et al., 2005), (2) using particle  
30 number size distribution and chemical composition data in separate and/or combined PMF  
31 runs (Beddows et al., 2015;Gu et al., 2011), (3) comparing PMF results with actual events  
32 during the study period (Ogulei et al., 2007), and (4) simply correlating the PMF results with  
33 gaseous pollutants data (Friend et al., 2013;Friend et al., 2012;Kim et al., 2004). It is



1 noteworthy that the major factors resolved by these studies have been nucleation, traffic,  
2 secondary aerosol, urban background, and wood burning.

3 Numerous studies have been performed in Los Angeles evaluating PM number  
4 concentrations as well as size distributions, with a focus on vehicular emissions as a major  
5 source of particle number in urban areas (Singh et al., 2006;Zhang et al., 2005). Source  
6 apportionment of atmospheric particles has also been extensively studied in Los Angeles, but  
7 almost all of the studies have focused on the contribution of different sources to PM mass  
8 rather than PM number concentration (Ham and Kleeman, 2011;Hasheminassab et al.,  
9 2013;Hwang and Hopke, 2006;Kim and Hopke, 2007;Kim et al., 2010;Schauer and Cass,  
10 2000). To the best of our knowledge, no source apportionment studies have ever been  
11 performed in Los Angeles on particle number size distributions using PMF. The only study  
12 providing a source apportionment of particle number concentrations in Los Angeles is that of  
13 Brines et al. (2015), in which major sources contributing to particle number concentrations  
14 were identified in five high-insolation cities around the world (Barcelona, Madrid, Roma, Los  
15 Angeles, and Brisbane) using the k-means clustering method. It should, however, be noted  
16 that, in case of Los Angeles, the Brines et al. (2015) study used particle number size  
17 distribution data for a rather limited time period (i.e., 3 months); moreover, the studied size  
18 distributions ranged from 13 nm to 400 nm, thus excluding potentially important PM sources  
19 contributing to the larger size fractions of PM<sub>2.5</sub> and/or PM<sub>10</sub>.

20 In the present work, we collected high-resolution (5-min measurements), wide-spectrum  
21 particle number size distribution data (i.e., 13 nm to 10 μm, covering the nucleation, Aitken,  
22 accumulation, and coarse PM modes) over a long period of time (i.e., 9 months, covering  
23 both warm and cold seasons) in a location near downtown of Los Angeles, California, to  
24 identify and quantify sources contributing to particle number concentrations using the most  
25 recent version of the PMF model (version 5.0). We also included gaseous pollutants (i.e., CO,  
26 NO, NO<sub>2</sub>, O<sub>3</sub>), particle mass (PM<sub>10-2.5</sub> and PM<sub>2.5</sub>), meteorological (temperature, relative  
27 humidity (RH), and wind speed), black carbon (BC), elemental carbon (EC) as well as  
28 primary (POC) and secondary organic carbon (SOC), and traffic (counts of light-duty  
29 vehicles (LDVs) and heavy-duty vehicles (HDVs)) data as inputs to help identify the factors  
30 resolved by the model. Results from the present study can be used as a platform for future  
31 health effect studies to estimate the source-specific impact of exposure to PM from a number  
32 concentration perspective, which is critical for development and establishment of abatement  
33 strategies and standards in order to minimize the most relevant health outcomes.

34



## 1 **2. Methodology**

### 2 *2.1. Sampling site*

3 Continuous measurements were carried out at the particle instrumentation unit (PIU)  
4 located on the University of Southern California's (USC) park campus, approximately 3 km  
5 south of downtown Los Angeles, CA. The PIU is located within approximately 150 m  
6 downwind of a routinely congested interstate freeway, i.e. I-110, and is also in close  
7 proximity to parking and construction facilities. Previous studies conducted by this research  
8 group have indicated that the PIU is a mixed urban site that is also heavily impacted by  
9 vehicular emissions (Geller et al., 2004; Moore et al., 2007; Hasheminassab et al., 2014b).

10

### 11 *2.2. Sampling time, method, and instrumentation*

12 Continuous measurements were conducted at the PIU from August 2014 through March  
13 2015 as well as in August 2015. To obtain number size distribution of atmospheric particles  
14 in the size range of 14 -760 nm (mobility diameter), a Scanning Mobility Particle Sizer  
15 (SMPS<sup>TM</sup>, TSI Model 3081) was used, which was connected to a Condensation Particle  
16 Counter (CPC, model 3020, TSI Inc., USA). Particles in the size range of 0.3-10  $\mu\text{m}$  (optical  
17 diameter) were measured using an Optical Particle Sizer (OPS<sup>TM</sup>, Model 3330, TSI Inc.,  
18 USA). The time resolution for these two instruments was 5 min. The OPS instrument was  
19 calibrated by the manufacturer using Polystyrene Latex (PSL) particles, which have a  
20 dynamic shape factor of 1 (i.e., spherical particles) and a refractive index of 1.59. It should  
21 also be noted that the measurements provided by the OPS instrument depend primarily on the  
22 refractive index and the dynamic shape factor (Hasheminassab et al., 2014b). Numerous  
23 studies have indicated that for spherical particles, the size selection offered by optical particle  
24 counters, such as the OPS instrument, is quite similar to the actual physical diameter of the  
25 particle being measured (Chen et al., 2011; Hasheminassab et al., 2014b; Hering and  
26 McMurry, 1991; Reid et al., 1994). That said, there is compelling evidence in the literature  
27 supporting the fact that the refractive index and the dynamic shape factor for ambient  
28 aerosols in urban areas (such as Los Angeles) are quite similar to those of PSL  
29 particles (Covert et al., 1990; Ebert et al., 2004; Hänel, 1968; Kent et al., 1983; Stolzenburg et  
30 al., 1998; Strawa et al., 2006; Watson et al., 2002). To further evaluate this assumption, we  
31 used the Multi-Instrument Manager (MIM<sup>TM</sup>) software, developed by TSI Inc., USA, which  
32 estimates the refractive index and dynamic shape factor of aerosols from parallel SMPS and  
33 OPS scans. The output from this software indicated that the average real part of the refractive  
34 index for the aerosols collected in this study was  $1.59 \pm 0.01$  and their dynamic shape factor



1 was  $0.99 \pm 0.02$ . This finding is also in concert with the results of Hasheminassab et al.  
2 (2014b), which reported an average shape factor of near unity at the same sampling site,  
3 using the apparent and material density of aerosols. Hence, further adjustment of OPS sizing  
4 was deemed unnecessary and the OPS size distribution, with the original size selection, was  
5 merged with the SMPS size spectra. More detailed information on the sensitivity of the OPS  
6 sizing to the refractive index and the dynamic shape factor of aerosols can be found in  
7 (Hasheminassab et al., 2014b).

8  
9 Black carbon (BC) concentrations, with a time resolution of 15 min, were measured  
10 using a portable Aethalometer (Magee scientific, model AE-42). Hourly concentrations of  
11 elemental carbon (EC) and organic carbon (OC) were measured using a semi-continuous  
12 EC/OC carbon aerosol analyzer (Model 4, Sunset Laboratory Inc., USA), using the  
13 thermal/optical transmittance measurement protocol of the National Institute of Occupational  
14 Safety and Health (NIOSH 5040). By applying the “EC tracer method”, Saffari et al. (2016)  
15 estimated the primary organic carbon (POC) and secondary organic carbon (SOC)  
16 concentrations from total OC at the same location. These two parameters (i.e., POC and  
17 SOC) were also used as input parameters in the PMF model, as they can provide valuable  
18 input regarding the detection of primary and secondary sources of PM. The EC tracer method  
19 has been discussed in detail elsewhere (Day et al., 2015; Saffari et al., 2016). Briefly, the main  
20 assumption in this method is that EC and POC are released from similar sources; therefore,  
21 this approach is most applicable where combustion is the main source of ambient POC (Day  
22 et al., 2015). It is noteworthy that, in the present study, the sampling site was located in close  
23 proximity to a major freeway, thereby making the EC tracer suitable for the data collected in  
24 this location, as it has also been used in previous studies in the same sampling site (Polidori et  
25 al., 2007; Saffari et al. 2016) as well as similar locations in the Los Angeles basin (Na et al.,  
26 2004; Strader et al., 1999). In this method, the following equations can be used after  
27 determining the ratio of POC to EC to estimate the concentration of SOC:

$$28 \quad \text{POC} = [\text{OC/EC}]_p \times \text{EC} + b \quad (1)$$

$$29 \quad \text{SOC} = \text{OC} - \text{POC} \quad (2)$$

30 where,  $[\text{OC/EC}]_p$  is the POC to EC ratio; b is the intercept of the linear regression between  
31 POC and EC, which is considered to be the portion of POC associated with non-combustion  
32 emissions. It is also noteworthy that we used the “high EC edge method” to determine



1 observations with a high probability of dominant POC contribution, which is believed to be a  
2 more accurate method for the identification of the  $[OC/EC]_p$  ratio compared to the traditional  
3 approach, as discussed by Day et al. (2015), and has also been successfully applied in a  
4 number of previous studies (Harrison and Yin, 2008; Lim and Turpin, 2002; Na et al. 2004).

5

### 6 2.3. Auxiliary variables

7 To help better identify the factors resolved by the PMF model, additional parameters,  
8 including gaseous pollutants (i.e., CO, NO, NO<sub>2</sub>, and O<sub>3</sub>) and particulate matter mass  
9 concentrations in two size fractions (i.e., PM<sub>10-2.5</sub> and PM<sub>2.5</sub>), meteorological parameters (i.e.,  
10 temperature, relative humidity, and wind speed), and traffic flow data (counts of LDVs and  
11 HDVs), were also included in the model as auxiliary variables. Hourly concentrations of  
12 particulate mass and gaseous pollutants together with hourly measurements of meteorological  
13 parameters were acquired from the online data base of California Air Resources Board  
14 (CARB), for the sampling site located in Downtown Los Angeles (North Main St.),  
15 approximately 3 km to the northeast of the PIU. The hourly traffic flow data were acquired  
16 from the nearest vehicle detection station (VDS) to our sampling site on the Freeway I-110,  
17 operated by the freeway performance measurement system (PeMS), under the  
18 California Department of Transportation (CalTrans). Table 1 provides a summary statistics of  
19 the input parameters to the PMF model in this study. To achieve the same time resolution  
20 across all variables, we calculated hourly-averaged data points for all variables.

21

### 22 2.4. Meteorology in central Los Angeles

23 To evaluate the impact of meteorological conditions on factor contributions as well as  
24 to better identify the resolved factors based on their expected seasonal trends, the study  
25 period was partitioned into two phases, i.e., colder phase (from November to February) and  
26 warmer phase (from August to October as well as March), and the model outputs, except for  
27 factor profiles, are presented for each phase accordingly. Figure 1 illustrates the diurnal  
28 variation of important meteorological parameters, namely, temperature, RH, wind speed, and  
29 solar radiation, in the cold and warm phases. As can be seen from the figure, on average,  
30 temperature was 5-7 °C higher in the warm phase than in the cold phase, although the trends  
31 were similar in both phases. Minimum temperatures were observed in the early morning  
32 (coinciding with morning rush hours), while maximum temperatures were seen at around  
33 noon. Conversely, RH peaked at night and exhibited a minimum in the early afternoon. RH



1 was also slightly higher in the warm phase than in the cold phase. As expected, wind speed  
2 peaked in the early afternoon during the warm phase and slightly shifted to the evening in the  
3 cold phase, while the slowest winds were blown during nighttime. The wind speeds were also  
4 higher in the warm phase compared to the cold phase. Solar radiation had a consistent trend  
5 in both phases, peaking at noon, with the levels being higher in the warm phase than in the  
6 cold phase, as one would expect. Similar trends and levels were also observed by  
7 Hasheminassab et al. (2014b) in central LA, indicating the occurrence of stable atmospheric  
8 conditions during nighttime until morning rush hours, especially in colder months of the year.

9

#### 10 2.5. PMF model

11 PMF, first developed by Paatero and Tapper (1993), is a multivariate statistical model  
12 used for identifying and quantifying the contribution of different sources to a set of samples  
13 using the fingerprints of those sources. This multivariate factor analysis tool decomposes a  
14 matrix of speciated data into two sub-matrices, i.e., factor profiles and source contributions,  
15 as shown below (Krecl et al., 2008):

$$16 \quad X = G \cdot F + E \quad (3)$$

17 where, X is the matrix of samples (here, particle number size distribution together with  
18 auxiliary variables data); G is the matrix containing source contributions; F is the matrix  
19 containing factor profiles; and E is the residual matrix.

20 The above equation can also be expressed mathematically, as the following (Norris et  
21 al., 2014):

$$22 \quad x_{ij} = \sum_{k=1}^p g_{ik} f_{kj} + e_{ij} \quad (4)$$

23 where,  $x_{ij}$  is the PM number concentration (or concentration of another auxiliary  
24 species) for the  $i$ th sample and the  $j$ th size bin (or species);  $p$  is the number of factors that  
25 contribute to the PM number concentrations;  $g_{ik}$  is the relative contribution of  $k$ th factor to  $i$ th  
26 sample;  $f_{kj}$  is the PM number concentration of  $j$ th size bin in the  $k$ th factor; and  $e_{ij}$  is the  
27 residual (observed–estimated) value for the  $i$ th sample and  $j$ th size bin.

28 With the constraint that no sample can have a significantly negative contribution and  
29 using a least-square method, the PMF then resolves factor profiles and contributions by  
30 attempting to minimize the Q value, as shown below (Paatero, 1997; Paatero and Tapper,  
31 1994):



$$Q = \sum_{i=1}^n \sum_{j=1}^m \left[ \frac{x_{ij} - \sum_{k=1}^p g_{ik} \cdot f_{kj}}{u_{ij}} \right]^2 \quad (5)$$

where,  $u_{ij}$  is the uncertainty associated with the sample  $x_{ij}$ .

One of the advantages of the PMF model is weighting every single value in the input data matrix using user-provided uncertainties, enabling the model to allow for measurement confidence in resolving the factor profiles and contributions (Paatero et al., 2014). In the present work, since no measurement uncertainties were available for the input parameters, we applied the method suggested by Ogulei et al. (2006a;2006b) and Zhou et al. (2014) to calculate the uncertainties for individual data points inserted into the model. For this purpose, measurement errors were first estimated for each data point using the following equation:

$$\sigma_{ij} = C_1(N_{ij} + \bar{N}_j) \quad (6)$$

where,  $\sigma_{ij}$  is the estimated measurement error for the  $i$ th sample and  $j$ th size bin (or concentration of auxiliary variables);  $C_1$  is an empirical constant usually between 0.01 and 0.05;  $N_{ij}$  is the observed number concentration for the  $i$ th sample and  $j$ th size bin (or concentration of auxiliary variables); and  $\bar{N}_j$  is the arithmetic mean of the PM number concentrations for the  $j$ th size bin (or concentration of auxiliary variables).

The value of the measurement method obtained from the above equation is then used to calculate the measurement uncertainty, according to the following equation:

$$S_{ij} = \sigma_{ij} + C_2 \max(|x_{ij}|, |y_{ij}|) \quad (7)$$

where,  $S_{ij}$  is the calculated uncertainty associated with the  $i$ th sample and  $j$ th size bin;  $C_2$  is an empirical constant usually between 0.1 and 0.5; and  $Y_{ij}$  is the value calculated by the model for  $x_{ij}$ . In the present work,  $C_1$  and  $C_2$  values of 0.05 and 0.1 were chosen to obtain the most physically interpretable solution using a trial and error approach.

In the present study, the most recent version of the PMF model, version 5.0, newly released by the United States Environmental Protection Agency (PMF guide), was used. Uncertainties associated with the resolved factor profiles were estimated using three error estimation methods, namely, Displacement (DISP) analysis, Bootstraps (BS) method, and a combination of DISP and BS methods (BS-DISP). For the DISP analysis, a solution was considered valid if the observed drop in the Q value was below 0.1% and there was no factor swaps for the smallest  $dQ_{\max}$  (i.e., 4). For the BS method, 100 runs were selected and a solution was considered valid if all of the factors had a mapping of above 90%. For the BS-



1 DISP analysis, a solution was considered valid if the observed drop in the Q value was below  
2 0.5% (Brown et al., 2015; Paatero et al., 2014).

3 The PMF model was run in the robust mode, which down-weights the effect of values  
4 with high uncertainties (i.e., values set as “weak” in the model) on the final solution resolved  
5 by the model (Brown et al., 2015). Missing values were replaced by interpolating the  
6 previous and the next data points in the matrix; however, to decrease the effect of these  
7 replaced values on the final solution, their uncertainty was set as three times the mean  
8 uncertainty for that species (that is practically what the model does to set a species as  
9 “weak”). Based on the recommendations presented by Brown et al. (2015), genuine zero  
10 values were included in the input matrix. Particle number concentration (PNC) was selected  
11 as the “total variable”, and the PMF model automatically turned it into a weak species by  
12 increasing its uncertainty by a factor of 3. An extra model uncertainty of 5% was also set to  
13 account for errors that are not covered in the input uncertainty values (Reff et al., 2007), since  
14 the uncertainty matrix only includes the effect of random as well as experimental errors.

15

## 16 *2.6. Input matrices*

17 The model was run in two different scenarios, one with EC/OC data, which included  
18 1053 samples of 131 species, and one without EC/OC data, which included 2976 samples of  
19 129 species. This was due mainly to the fact that the EC/OC data were being collected in  
20 parallel for a different study that coincided with the current work in a span of time shorter  
21 than the entire study period. Therefore, in order to keep the large number of samples from the  
22 main study (i.e., 2976) as well as to use the critical advantage of having EC/OC data in the  
23 factor identification process, it was decided to run the PMF model in two different scenarios,  
24 one including EC/OC data and one without these data. It should also be noted that although  
25 the latter matrix contained BC data, this variable was excluded from the former matrix to  
26 avoid double counting, as EC was already included in the dataset. The results of the PMF run  
27 including the EC/OC data are provided in the supplementary information (Figure S1).

28

29

## 30 **3. Results and discussion**

### 31 *3.1. Overview of the data*

32 Table 2 presents the statistical characteristics of the species included in the PMF model.  
33 In this table, signal-to-noise (S/N) ratio is a parameter that indicates if the variability in the  
34 measurements is real or within the data noise. In the current version of the model, i.e., PMF



1 5.0, the method used for calculating the S/N ratio has been updated compared to the previous  
2 versions, resolving the disadvantages associated with the previous method of S/N calculation  
3 (for a more detailed discussion on the S/N calculation methods, see SI). In the current  
4 method, if the resulting S/N ratio is above 1, it can be concluded that the species has a  
5 reliable signal. As reported in Table 2, all the species in the input matrix had S/N ratios well  
6 above 1, indicating very strong signals for all the variables. Figure S2 also illustrates the  
7 correlation between the measured and PMF-predicted total number concentrations for the  
8 entire sampling period. As can be seen in the figure, the high correlation between measured  
9 and predicted values ( $R^2=0.99$ ) and very close to 1 slope of the regression line indicate that  
10 the PMF model has been successful in modeling the input data and apportioning the total PM  
11 number concentrations to the resolved factors.

12 Figure 2 depicts the average number and volume size distributions of all the input data  
13 to the PMF model by phase, which were collected during the entire study period. As shown in  
14 the figure, the vast majority of the particles were smaller than 100 nm, and the number  
15 concentration had a mode diameter at around 40 nm. Additionally, a significantly higher  
16 number concentration was observed in the cold phase compared to the warm phase, which is  
17 consistent with the results from the previous studies conducted in Los Angeles (Hudda et al.,  
18 2010; Singh et al., 2006). Regarding volume concentrations, we observed one minor volume  
19 mode at the size range of 300-500 nm and a major mode at around 4-6  $\mu\text{m}$ . In this case, the  
20 volume concentration was higher in the cold phase than in the warm phase for the minor  
21 mode diameter (at 300-500 nm), while a sharper peak was observed for the major mode  
22 diameter (at around 4-6  $\mu\text{m}$ ) in the warm phase compared to the cold phase. This PM volume  
23 size distribution is typical of urban areas (Vu et al., 2015), and is also consistent with the  
24 findings of a previous study conducted recently by this research group at the same sampling  
25 location (Hasheminassab et al., 2014b).

26

### 27 3.2. Number of Factors

28 In the present work, the PMF model was run several times using different number of  
29 factors, input uncertainty matrices (as noted in the methods section), and extra modeling  
30 uncertainties to obtain the best and most physically applicable solution. Additionally, we used  
31 several criteria to determine the best solution resolved by the model, including: 1) particle  
32 number size distribution profiles for different factors; 2) volume size distribution profiles for  
33 the resolved factors; 3) profiles of auxiliary variables for different factors; 4) contribution of  
34 each factor in different seasons to the total number concentrations; 5) diurnal variations of



1 each of the resolved factors in the cold and warm phases; 6) diurnal variations of each of the  
2 resolved factors in weekdays versus weekends; and 7) correlation between auxiliary variables  
3 and the relative contribution of each of the resolved factors. The six-factor solution was  
4 found to present the most physically explainable one, and was, therefore, chosen as the final  
5 solution. When the model was run with one less factor (i.e., 5-factor solution), the model  
6 could not distinguish the two traffic factors, and Traffic 1 and Traffic 2 factors were merged  
7 together. On the other hand, when the model was run with one more factor (i.e., 7-factor  
8 solution), a new factor was resolved by the model, having a mode diameter between that of  
9 “urban background aerosol” and “secondary aerosol”, but without having any distinct diurnal,  
10 seasonal, or weekday/weekend trends or auxiliary variables profile. Therefore, this factor  
11 could not be meaningfully interpreted and identified, prompting us to choose the 6-factor as  
12 the optimal solution.

13 Figure 3 illustrates the number size distributions as well as the auxiliary variables  
14 profiles for each of the factors resolved by the PMF. Figure 4 indicates volume size  
15 distribution of each factor. In Figures 3, 4, and S1, the black solid lines represent absolute  
16 concentrations (number or volume) of each size bin and should be read from the left Y axis,  
17 while the grey triangles represent the explained variation of each size bin and should be read  
18 from the right Y axis. The relative contributions (overall, and by cold or warm phases) of  
19 each factor to the total number concentrations are shown in Figure 5. Figure 6 illustrates the  
20 contribution (particles/cm<sup>3</sup>) of each of the PMF-resolved factors to the total number  
21 concentrations in the cold and warm phases within box and whisker plot. The diurnal  
22 variations and the weekday/weekend trends (geometric means) for each of the factors are  
23 illustrated in Figures 7 and 8, respectively. The spearman correlation coefficient matrix  
24 indicating the association between the auxiliary variables and the factors resolved by the  
25 PMF model is also presented in Table 3.

26

### 27 3.3. Factor identification

28 *Factor 1:* Factor 1 has a number mode at <20 nm, a volume mode at <20 nm, and  
29 contributes 17.3% (11.7-24%) to the total number concentrations (Figures 3, 4, and 5). This  
30 factor has strong positive (except for RH, with which this factor has negative correlation)  
31 associations with temperature, wind speed, SOC, and O<sub>3</sub> (Table 3), which are also  
32 statistically significant (p<0.05). These associations are also apparent from high loadings of  
33 temperature, RH, wind speed, and O<sub>3</sub> in the auxiliary variables profile (Figures 3 and S1).  
34 The contribution of this factor to the total number concentration was also higher in the warm



1 phase than in the cold phase, when higher temperatures, wind speeds, and solar radiation are  
2 observed (Figure 1); this was the case both in terms of percent contribution (24% in the warm  
3 phase vs. 11.7% in the cold phase) and number concentration ( $589\pm 25$  particles/cm<sup>3</sup> in the  
4 cold phase vs.  $1153\pm 28$  particles/cm<sup>3</sup> in the warm phase) (Figures 5 and 6 and Table S1). The  
5 diurnal variations for this factor also revealed a sharp peak in the afternoon (2-6 PM) (Figure  
6 7), which coincides with very high temperatures, wind speeds, and solar radiation as well as  
7 with minimum RH (Figure 1). However, there was no significant distinction in the diurnal  
8 variation patterns of this factor in weekdays compared to weekends (Figure 8).

9 The above characteristics are all typical of a "nucleation" factor, during which new  
10 particles are formed via photochemical events under high temperatures, high wind speeds,  
11 and low RH (Beddows et al., 2015; Brines et al., 2015; Dall'Osto et al., 2012; Vu et al., 2015).  
12 Our findings are most specifically consistent with those of the study of Brines et al. (2015), in  
13 which the authors had reported nucleation as one of the major sources of UFPs in five high-  
14 insolation cities, including Los Angeles using the data obtained from the same sampling  
15 location. They observed very similar diurnal variation for nucleation, with peaks in early  
16 afternoon at the same sampling location in Los Angeles.

17

18 *Factor 2:* Factor 2 is mostly represented by particles at 20-40 nm and contributes about  
19 40% (33.2-43.4%) to the total number concentration (Figures 3 and 5). It also has a volume  
20 concentration peak at around 30-40 nm (Figure 4). Judging by the loadings presented in the  
21 auxiliary variables profile (Figures 3) and correlation coefficients presented in Table 3, this  
22 factor has clear associations with gaseous pollutants (e.g., CO, NO, and NO<sub>2</sub>), BC, EC, and  
23 POC (from the scenario containing EC/OC data (Figure S1), which themselves are indicators  
24 of vehicular emissions (Gu et al., 2011; Ogulei et al., 2006b). In addition, high species  
25 loadings (Figure 3) and correlation coefficients (Table 3) of LDV and HDV counts can also  
26 be observed for this factor, indicating the influence of nearby passing traffic on this factor.  
27 The contribution of this factor to the total number concentration was also much higher in the  
28 cold phase than in the warm phase, when lower temperatures, wind speeds, and solar  
29 radiation (Figure 1) lead to increased atmospheric stability and lower mixing height  
30 (Hasheminassab et al., 2014a); this was the case both in terms of percent contribution (43.4%  
31 in the cold phase vs. 33.2% in the warm phase) and number concentration ( $3166\pm 66$   
32 particles/cm<sup>3</sup> in the cold phase vs.  $1201\pm 61$  particles/cm<sup>3</sup> in the warm phase) (Figures 5 and 6  
33 and Table S1). The diurnal variations also revealed a distinctive pattern peaking in the  
34 morning rush hours (around 7-8 AM) (Fig. 7). The weekday/weekend analysis also indicated



1 that this factor had higher contributions during the weekdays compared to the weekends  
2 (Figure 8). Therefore, this factor can be attributed to traffic tailpipe emissions. Previous  
3 source apportionment studies on number size distributions have also associated such  
4 characteristics with fresh vehicular emissions (Beddows et al., 2015; Dall'Osto et al., 2012; Vu  
5 et al., 2015). This factor is denoted as “traffic 1”, given that another factor attributed to traffic  
6 emissions was resolved, which will be discussed in the following section. The characteristics  
7 of this traffic factor are in agreement with what Brines et al. (2015) reported for five high-  
8 insolation cities, including Los Angeles.

9  
10 *Factor 3:* This factor has a major peak in the Aitken mode (60-100 nm) and contributes  
11 27.5% (25-27.6%) to the total number concentration (Figures 3 and 5). It also exhibited a  
12 volume concentration peak at around 100 nm (Figure 4). Judging by the loadings presented in  
13 the auxiliary variables profile (Figures 3 and S1) and correlation coefficients presented in  
14 Table 3, significant associations can be observed between this factor and gaseous pollutants  
15 (e.g., CO, NO, and NO<sub>2</sub>), as well as with BC (and EC from the scenario containing EC/OC  
16 data (Fig. S1)). Although weaker than those of Factor 2, there are significant positive  
17 associations between this factor and LDV and HDV counts (Figure 3 and Table 3),  
18 suggesting the likely influence of nearby passing traffic. This factor also had a significantly  
19 higher contribution to the total number concentrations in the cold phase than in the warm  
20 phase (an average of 1755±56 particles/cm<sup>3</sup> in the cold phase vs. 1059±43 particles/cm<sup>3</sup> in  
21 the warm phase (Figure 6)), in spite of the fact that its percent contribution to the total PM  
22 number concentrations was comparable in both phases, and slightly higher in the warm phase  
23 (25% in the cold phase vs. 27.6% in the warm phase (Figure 5)). This is due mainly to the  
24 fact that the contribution of the "traffic 1" factor is so large in the cold phase that has  
25 significantly obscured the percent contribution of other factors in this phase, even though  
26 their absolute contributions in terms of total number concentrations were higher in the cold  
27 phase.

28 The diurnal variations for this factor also indicated clear peaks during the morning rush  
29 hours (6-8 am) in both phases, along with another peak at late night during the cold phase,  
30 most likely due to the stagnant atmospheric conditions during this time of the year, which  
31 traps the emissions in lower altitudes (Figure 7). The weekday/weekend analysis for this  
32 factor revealed larger contributions in weekdays than in weekends, especially during daytime  
33 hours. The slightly higher nighttime contribution of this factor in the weekends compared to  
34 the weekdays can be attributed to the larger number of within-city travels being made on



1 holiday nights. These levels and trends are, overall, suggestive of emissions from vehicular  
2 sources. However, the larger size range of this factor compared to factor 2, combined with the  
3 involvement of EC and SOC (as observed from the scenario containing EC/OC data (Fig.  
4 S1)) as well as BC, suggest that although this factor also originates from “traffic”, the  
5 particles are “older” (i.e., more aged) than those observed in factor 2 and are mostly in the  
6 Aitken and Accumulation modes; therefore, it was labeled as "traffic 2". This finding is also  
7 consistent with those of the previous studies (e.g., Brines et al. (2015)), in which the authors  
8 detected distinct traffic factors (with a collective relative contribution of approximately 60%  
9 in Los Angeles at the same sampling site) using a different source apportionment method,  
10 named k-means cluster analysis. It should be noted that it is quite common in source  
11 apportionment studies performed on size-segregated PM number concentrations to detect  
12 more than one traffic factors, due primarily to the fact that particle sizes may change, as  
13 particles undergo processes including agglomeration as well as evaporation or condensation  
14 of semi-volatile species from- or onto their surface following their release in the atmosphere  
15 (Harrison et al., 2016;Kim et al., 2004;Zhou et al., 2005).

16 It is also noteworthy that the traffic 2 factor has a slightly higher HDV loading than  
17 traffic 1 factor (Figures 3 and S1). It also has a somewhat stronger positive correlation with  
18 HDV ( $R=0.43$ ) than with LDV ( $R=0.41$ ), while the traffic 1 factor has a stronger correlation  
19 with LDV ( $R=0.69$ ) than with HDV ( $R=0.52$ ). Additionally, the stronger correlation of traffic  
20 2 factor with EC and BC compared to traffic 1 leads us to the hypothesis that HDV might be  
21 contributing more to this factor than LDV is. Vu et al. (2015) have also suggested that  
22 observing a number concentration mode at the size range of 60-100 nm can be a result of  
23 incomplete combustion of diesel fuel, consisting of pyrolytic EC and OC. Other studies have  
24 also found two particle modes, or factors, for traffic-related emissions. Although the  
25 emissions in both of these two modes are believed to come from the same fleet of vehicles,  
26 they have different formation mechanisms and chemistry, with particles associated with the  
27 second mode (i.e., soot mode) assumed to have an elemental carbon core. This is consistent  
28 with the findings of the present study, judging by the mode diameter and high loading of BC,  
29 EC, and OC in the traffic 2 factor (Figures 3 and S1) and the strong correlation of this factor  
30 with BC, EC, and OC (Table 3). Additionally, studies have indicated that a fraction of diesel  
31 PM emissions, which is generally in the range of 50-200 nm, comprises particles that have an  
32 elemental core, with low-vapor-pressure hydrocarbons and sulfur compounds being adsorbed  
33 on their surface (Burtcher, 2005). Therefore, it might be likely that this factor is representing



1 a higher contribution of HDV emissions, although stronger evidence is required to confirm  
2 this hypothesis.

3

4 *Factor 4:* Factor 4, which contributes 12.2% (7.4-17.1%) to the total number  
5 concentration, is represented by a number mode at around 220 nm and a volume mode at  
6 around 250 nm (Figures 3, 4, and 5). The profile for the auxiliary variables also indicates  
7 high loadings for gaseous pollutants (e.g., CO, NO, and NO<sub>2</sub>) and BC (Figure 3) as well as  
8 for EC and SOC (when the PMF model was run with the EC/OC data (Fig. S1)). The large  
9 correlation coefficients of this factor with the aforementioned species also confirm its strong  
10 association with these parameters (Table 3). The lower-than-unity NO/NO<sub>2</sub> ratio for this  
11 factor also suggests that these particles are aged compared to the newly formed particles (Liu  
12 et al., 2014). This is also supported by the stronger positive correlation of this factor with  
13 SOC than with POC, suggesting the fact that this factor is not coming from direct emissions  
14 and has most likely undergone processes and reactions in the atmosphere. As can be inferred  
15 from Figures 5 and 6, the contribution of this factor is significantly higher in the cold phase  
16 than in the warm phase, both in terms of percent contribution (17.1% in the cold phase vs.  
17 7.4% in the warm phase) and the absolute contribution to the total number concentration  
18 (1200±41 particles/cm<sup>3</sup> in the cold phase vs. 284±23 particles/cm<sup>3</sup> in the warm phase). As  
19 seen in Figure 7, the diurnal variations for this factor also exhibit a clear peak during morning  
20 hours, which indicates higher concentrations when atmosphere is more stable and wind  
21 speeds are low, especially in the cold phase when these conditions are even more intense  
22 (Figure 1). The weekday/weekend analysis also revealed a slightly elevated contribution of  
23 this factor to the total number concentrations during morning rush hours, especially during  
24 the weekdays, suggesting the small influence of traffic emissions on this factor. Previous  
25 studies have indicated that these are characteristics of the “urban background aerosol”, as  
26 suggested by (Beddows et al., 2015; Dall'Osto et al., 2012).

27

28 *Factor 5:* Factor 5 has a number and volume mode at around 500 nm and a minor  
29 number mode at 50 nm (looking at the black dots, representing the explained variations)  
30 (Figures 3 and 4). This factor contributes 2.1% (1.5-2.5%) to the total number concentration  
31 (Figure 5). It is also associated with high loadings of PM<sub>2.5</sub> mass concentration (i.e., major  
32 contributor to PM<sub>2.5</sub> mass), NO, NO<sub>2</sub>, Temperature, RH (Figure 3), and SOC (as observed  
33 from the scenario containing EC/OC data (Figure S1)). This is also supported by the results  
34 of the correlation analysis presented in Table 3, indicating that this factor has strong positive



1 correlations with  $PM_{2.5}$ , NO,  $NO_2$ , Temperature, RH, and SOC. The overall small  
2 contribution of this factor to the total number concentration was slightly higher in the cold  
3 phase than in the warm phase; this was the case both in terms of percent contribution (2.5%  
4 in the cold phase vs. 1.5% in the warm phase) and number concentration ( $111 \pm 11$   
5 particles/cm<sup>3</sup> in the cold phase vs.  $100 \pm 5$  particles/cm<sup>3</sup> in the warm phase) (Figures 5 and 6  
6 and Table S1). The diurnal variation for this factor also reveals a significant increase during  
7 nighttime, especially during the cold phase (Figure 7). However, the weekday/weekend  
8 analysis did not reveal any distinctive trend pertaining to the day of the week for this factor  
9 (Figure 8). These pieces of evidence point to “secondary aerosols” as the most appropriate  
10 title for this factor, which is consistent with the results of previous PMF studies both on  
11 number size distributions and chemical speciation data (Beddows et al., 2015; Hasheminassab  
12 et al., 2014a). Table 3 indicates a much higher correlation of this factor with SOC than POC  
13 (R values of 0.5 and 0.2, respectively). The association of this factor with RH and  
14 temperature, along with its higher contribution to particle number during the cold phase,  
15 particularly at night, support the hypothesis that this factor likely represents the fraction of  
16 aerosols produced by secondary reactions on a regional scale, including ammonium nitrate  
17 (whose partitioning in the PM phase increases with decreasing temperature and increased  
18 RH), but also secondary organic aerosols from nighttime and/or aqueous phase reactions, as  
19 indicated in earlier studies in this area (Hersey et al., 2011; Venkatachari et al., 2005). In a  
20 previous source apportionment study on  $PM_{2.5}$  chemical speciation data in downtown Los  
21 Angeles, we also found a similar factor profile, representing a mixture of secondary  
22 components (dominated by secondary nitrate and SOC) with higher contribution during the  
23 cold season (Hasheminassab et al., 2014a). Moreover, previous studies have shown that  
24 secondary organic aerosol formed at nighttime together with ammonium nitrate are major  
25 contributors to the mass concentrations of  $PM_{2.5}$ , which was also observed in the present  
26 work from the high loading of  $PM_{2.5}$  mass concentration in this profile (Figure 3)  
27 (Hasheminassab et al., 2014a; Arhami et al., 2010; Saffari et al., 2016).

28

29 *Factor 6:* Factor 6 is dominated by particles at around 1  $\mu m$  and above (Figure 3). This  
30 factor also had a volume mode at  $> 1 \mu m$  (Figure 4). Although this factor contributes only  
31 1.1% (0.2-6.3%) to the total number concentration (Figure 5), it is associated with high  
32 loadings of coarse PM and  $PM_{2.5}$  (great contributor to mass) (Figure 3). In addition, high  
33 loadings of temperature and wind speed were observed for this factor (Figure 3). Table 3 also  
34 indicates strong correlation of this factor with coarse PM,  $PM_{2.5}$ , temperature, and wind



1 speed. The contribution of this factor to the total number concentration was also higher in the  
2 warm phase than in the cold phase, both in terms of percent contribution (0.2% in the cold  
3 phase vs. 6.3% in the warm phase) and number concentration ( $14\pm 1$  particles/cm<sup>3</sup> in the cold  
4 phase vs.  $243\pm 3$  particles/cm<sup>3</sup> in the warm phase) (Figures 5 and 6 and Table S1). The diurnal  
5 variations for this factor exhibited significantly higher contributions during daytime,  
6 especially in the warm phase (Figure 7), when atmosphere is unstable, wind speed is high,  
7 and the mixing height is at its maximum (Figure 1). However, the weekday/weekend analysis  
8 did not reveal any distinctive trend pertaining to the day of the week for this factor (Figure 8).  
9 Based on all of the abovementioned characteristics, this factor was named “soil/road dust”  
10 (Gietl et al., 2010; Harrison and Booker, 2001; Harrison et al., 2012). This is also quite  
11 consistent with the findings of the study of Hasheminassab et al. (2014a), in which the  
12 authors apportioned the sources of ambient fine particulate matter across the state of  
13 California. In that study, the authors observed a lower contribution of the soil factor to  
14 particle mass concentrations in the northern regions of the state of California, mainly because  
15 of higher RH and increased precipitation that inhibit the re-suspension of soil due to strong  
16 winds (Harrison and Booker, 2001). In the present study, similarly, the contribution of this  
17 factor was higher in the warm phase, when higher temperatures and wind speeds facilitate the  
18 re-suspension of soil and dust (Figure 1).

19

#### 20 **4. Summary and conclusions**

21 The present study was the first attempt to characterize major sources of PM number  
22 concentrations and quantify their contributions using the PMF receptor model applied on PM  
23 number size distributions in the range of 13 nm to 10 μm combined with several auxiliary  
24 variables, including BC, EC/OC, PM mass, gaseous pollutants, meteorological, and traffic  
25 flow data, in central Los Angeles. The six-factor solution was found to be the most physically  
26 applicable solution for the input data: nucleation, traffic 1, traffic 2, urban background  
27 aerosol, secondary aerosol, and soil. Traffic sources (1 and 2) were the major contributor to  
28 PM number concentrations, making up to above 60% of the total number concentrations  
29 combined, with larger contributions in the cold phase compared to the warm phase, when  
30 lower temperatures, wind speeds, and solar radiation lead to increased atmospheric stability  
31 and lower mixing height. The contribution of traffic factors was largest during morning and  
32 afternoon rush hours; it was also higher in the weekdays compared to the weekends, as  
33 expected. In agreement with the findings of previous studies in Los Angeles, nucleation was



1 another major factor contributing to the total number concentrations (17%), having a larger  
2 contribution in the warm phase than in the cold phase. The diurnal variations for this factor  
3 also revealed a sharp peak in the afternoon (2-6 PM), which coincides with high  
4 temperatures, wind speeds, and solar radiation as well as with minimum RH, providing ideal  
5 conditions for the occurrence of photochemical nucleation processes, especially during  
6 warmer seasons. Urban background aerosol, secondary aerosol, and soil, with relative  
7 contributions of approximately 12%, 2.1%, and 1.1%, respectively, overall accounted for  
8 approximately 15% of PM number concentrations. However, these factors dominated the PM  
9 volume and mass concentrations, due mainly to their larger mode diameters.

10

### 11 **Acknowledgement**

12 The authors wish to acknowledge the support from the USC Viterbi School of Engineering's  
13 Ph.D. fellowship award.

14

### 15 **References**

- 16 Alleman, L. Y., Lamaison, L., Perdrix, E., Robache, A., and Galloo, J.-C.: PM 10 metal  
17 concentrations and source identification using positive matrix factorization and wind  
18 sectoring in a French industrial zone, *Atmos. Res.*, 96, 612-625, 2010.
- 19 Arhami, M., Minguillón, M. C., Polidori, A., Schauer, J. J., Delfino, R. J., and Sioutas, C.:  
20 Organic compound characterization and source apportionment of indoor and outdoor  
21 quasi-ultrafine particulate matter in retirement homes of the Los Angeles Basin, *Indoor*  
22 *Air*, 20, 17-30, 2010.
- 23 Beddows, D. C. S., Harrison, R. M., Green, D. C., and Fuller, G. W.: Receptor modelling of  
24 both particle composition and size distribution from a background site in London, UK,  
25 *Atmos. Chem. Phys. Discuss.*, 15, 10123-10162, 2015.
- 26 Brines, M., Dall'Osto, M., Beddows, D. C. S., Harrison, R. M., Gómez-Moreno, F., Núñez,  
27 L., Artíñano, B., Costabile, F., Gobbi, G. P., and Salimi, F.: Traffic and nucleation  
28 events as main sources of ultrafine particles in high-insolation developed world cities,  
29 *Atmos. Chem. Phys.*, 15, 5929-5945, 2015.
- 30 Brook, R. D., Rajagopalan, S., Pope, C. A., Brook, J. R., Bhatnagar, A., Diez-Roux, A. V.,  
31 Holguin, F., Hong, Y., Luepker, R. V., and Mittleman, M. A.: Particulate matter air  
32 pollution and cardiovascular disease an update to the scientific statement from the  
33 American Heart Association, *Circulation*, 121, 2331-2378, 2010.
- 34 Brown, S. G., Eberly, S., Paatero, P., and Norris, G. A.: Methods for estimating uncertainty in  
35 PMF solutions: Examples with ambient air and water quality data and guidance on  
36 reporting PMF results, *Sci. total environ.*, 518, 626-635, 2015.
- 37 Brunekreef, B., and Forsberg, B.: Epidemiological evidence of effects of coarse airborne  
38 particles on health, *Eur. Respir. J.*, 26, 309-318, 2005.
- 39 Burtscher, H.: Physical characterization of particulate emissions from diesel engines: a  
40 review, *J. Aerosol Sci.*, 36, 896-932, 2005.
- 41 Chen, G., Ziemba, L. D., Chu, D. A., Thornhill, K. L., Schuster, G. L., Winstead, E. L.,  
42 Diskin, G. S., Ferrare, R. A., Burton, S. P., and Ismail, S.: Observations of Saharan dust



- 1 microphysical and optical properties from the Eastern Atlantic during NAMMA  
2 airborne field campaign, *Atmos. Chem. Phys.*, 11, 723-740, 2011.
- 3 Chen, L. C., Peoples, S. M., and Amdur, M. O.: Pulmonary effects of sulfur oxides on the  
4 surface of copper oxide aerosol, *Am. Ind. Hyg. Assoc. J.*, 52, 187-191, 1991.
- 5 Covert, D. S., Heintzenberg, J., and Hansson, H.-C.: Electro-optical detection of external  
6 mixtures in aerosols, *Aerosol Sci. Tech.*, 12, 446-456, 1990.
- 7 Dall'Osto, M., Beddows, D. C. S., Pey, J., Rodriguez, S., Alastuey, A., Harrison, R. M., and  
8 Querol, X.: Urban aerosol size distributions over the Mediterranean city of Barcelona,  
9 NE Spain, *Atmo. Chem. Phys.*, 12, 10693-10707, 2012.
- 10 Davis, D. A., Bortolato, M., Godar, S. C., Sander, T. K., Iwata, N., Pakbin, P., Shih, J. C.,  
11 Berhane, K., McConnell, R., and Sioutas, C.: Prenatal exposure to urban air  
12 nanoparticles in mice causes altered neuronal differentiation and depression-like  
13 responses, 2013.
- 14 Day, M. C., Zhang, M., and Pandis, S. N.: Evaluation of the ability of the EC tracer method  
15 to estimate secondary organic carbon, *Atmos. Environ.*, 112, 317-325, 2015.
- 16 Delfino, R. J., Sioutas, C., and Malik, S.: Potential role of ultrafine particles in associations  
17 between airborne particle mass and cardiovascular health, *Environ. health perspect.*,  
18 934-946, 2005.
- 19 Delfino, R. J., Tjoa, T., Gillen, D. L., Staimer, N., Polidori, A., Arhami, M., Jamner, L.,  
20 Sioutas, C., and Longhurst, J.: Traffic-related Air Pollution and Blood Pressure in  
21 Elderly Subjects With Coronary Artery Disease, *Epidemiology (Cambridge, Mass.)*, 21,  
22 2010.
- 23 Dockery, D. W., and Stone, P. H.: Cardiovascular risks from fine particulate air pollution, *N.*  
24 *Engl. J. Med.*, 356, 511-513, 2007.
- 25 Donaldson, K., Li, X. Y., and MacNee, W.: Ultrafine (nanometre) particle mediated lung  
26 injury, *J. Aerosol Sci.*, 29, 553-560, 1998.
- 27 Dreher, K. L., Jaskot, R. H., Lehmann, J. R., Richards, J. H., Ghio, J. K. M. A. J., and Costa,  
28 D. L.: Soluble transition metals mediate residual oil fly ash induced acute lung injury, *J.*  
29 *Toxicol. Environ. Health A*, 50, 285-305, 1997.
- 30 Dutton, S. J., Vedal, S., Piedrahita, R., Milford, J. B., Miller, S. L., and Hannigan, M. P.:  
31 Source apportionment using positive matrix factorization on daily measurements of  
32 inorganic and organic speciated PM 2.5, *Atmos. Environ.*, 44, 2731-2741, 2010.
- 33 Ebert, M., Weinbruch, S., Hoffmann, P., and Ortner, H. M.: The chemical composition and  
34 complex refractive index of rural and urban influenced aerosols determined by  
35 individual particle analysis, *Atmos. Environ.*, 38, 6531-6545, 2004.
- 36 Friend, A. J., Ayoko, G. A., Jayaratne, E. R., Jamriska, M., Hopke, P. K., and Morawska, L.:  
37 Source apportionment of ultrafine and fine particle concentrations in Brisbane,  
38 Australia, *Environ. Sci. Pollut. R.*, 19, 2942-2950, 2012.
- 39 Friend, A. J., Ayoko, G. A., Jager, D., Wust, M., Jayaratne, E. R., Jamriska, M., and  
40 Morawska, L.: Sources of ultrafine particles and chemical species along a traffic  
41 corridor: comparison of the results from two receptor models, *Environ. Chem.*, 10, 54-  
42 63, 2013.
- 43 Gauderman, W. J., Urman, R., Avol, E., Berhane, K., McConnell, R., Rappaport, E., Chang,  
44 R., Lurmann, F., and Gilliland, F.: Association of improved air quality with lung  
45 development in children, *N. Engl. J. Med.*, 372, 905-913, 2015.
- 46 Geller, M. D., Fine, P. M., and Sioutas, C.: The relationship between real-time and time-  
47 integrated coarse (2.5–10  $\mu\text{m}$ ), intermodal (1–2.5  $\mu\text{m}$ ), and fine (< 2.5  $\mu\text{m}$ ) particulate  
48 matter in the Los Angeles Basin, *J. Air . Waste Manage. Assoc.*, 54, 1029-1039, 2004.



- 1 Gietl, J. K., Lawrence, R., Thorpe, A. J., and Harrison, R. M.: Identification of brake wear  
2 particles and derivation of a quantitative tracer for brake dust at a major road, *Atmos.*  
3 *Environ.*, 44, 141-146, 2010.
- 4 Gu, J., Pitz, M., Schnelle-Kreis, J., Diemer, J., Reller, A., Zimmermann, R., Soentgen, J.,  
5 Stoelzel, M., Wichmann, H. E., and Peters, A.: Source apportionment of ambient  
6 particles: comparison of positive matrix factorization analysis applied to particle size  
7 distribution and chemical composition data, *Atmos. Environ.*, 45, 1849-1857, 2011.
- 8 Ham, W. A., and Kleeman, M. J.: Size-resolved source apportionment of carbonaceous  
9 particulate matter in urban and rural sites in central California, *Atmos. Environ.*, 45,  
10 3988-3995, 2011.
- 11 Hänel, G.: The real part of the mean complex refractive index and the mean density of  
12 samples of atmospheric aerosol particles, *Tellus*, 20, 371-379, 1968.
- 13 Harrison, R. M., and Yin, J.: Sources and processes affecting carbonaceous aerosol in central  
14 England, *Atmos. Environ.*, 42, 1413-1423, 2008.
- 15 Harrison, R. M., Beddows, D. C. S., and Dall'Osto, M.: PMF analysis of wide-range particle  
16 size spectra collected on a major highway, *Environ. sci. tech.*, 45, 5522-5528, 2011.
- 17 Harrison, R. M., Jones, A. M., Gietl, J., Yin, J., and Green, D. C.: Estimation of the  
18 contributions of brake dust, tire wear, and resuspension to nonexhaust traffic particles  
19 derived from atmospheric measurements, *Environ. sci. tech.*, 46, 6523-6529, 2012.
- 20 Harrison, R. M., Jones, A. M., Beddows, D. C. S., Dall'Osto, M., and Nikolova, I.:  
21 Evaporation of traffic-generated nanoparticles during advection from source, *Atmos.*  
22 *Environ.*, 125, Part A, 1-7, 2016.
- 23 Harrison, R. M., Yin, J., Mark, D., Stedman, J., Appleby, R. S., and Booker, J., and  
24 Moorcroft, S.: Studies of the coarse particle (2.5–10  $\mu\text{m}$ ) component in UK urban  
25 atmospheres, *Atmos. Environ.*, 35, 3667–3679, 2001.
- 26 Hasheminassab, S., Daher, N., Schauer, J. J., and Sioutas, C.: Source apportionment and  
27 organic compound characterization of ambient ultrafine particulate matter (PM) in the  
28 Los Angeles Basin, *Atmos. Environ.*, 79, 529-539, 2013.
- 29 Hasheminassab, S., Daher, N., Saffari, A., Wang, D., Ostro, B. D., and Sioutas, C.: Spatial  
30 and temporal variability of sources of ambient fine particulate matter (PM<sub>2.5</sub>) in  
31 California, *Atmos. Chem. Phys.*, 14, 12085-12097, 2014a.
- 32 Hasheminassab, S., Pakbin, P., Delfino, R. J., Schauer, J. J., and Sioutas, C.: Diurnal and  
33 seasonal trends in the apparent density of ambient fine and coarse particles in Los  
34 Angeles, *Environ. Pollut.*, 187, 1-9, 2014b.
- 35 Hering, S. V., and McMurry, P. H.: Optical counter response to monodisperse atmospheric  
36 aerosols, *Atmos. Environ.*, 25, 463-468, 1991.
- 37 Hersey, S. P., Craven, J. S., Schilling, K. A., Metcalf, A. R., Sorooshian, A., Chan, M. N.,  
38 Flagan, R. C., and Seinfeld, J. H.: The Pasadena Aerosol Characterization Observatory  
39 (PACO): chemical and physical analysis of the Western Los Angeles basin aerosol,  
40 *Atmos. Chem. Phys.*, 11, 7417-7443, 2011.
- 41 Hudda, N., Cheung, K., Moore, K. F., and Sioutas, C.: Inter-community variability in total  
42 particle number concentrations in the eastern Los Angeles air basin, *Atmos. Chem. and*  
43 *Phys.*, 10, 11385-11399, 2010.
- 44 Hwang, I., and Hopke, P. K.: Comparison of source apportionments of fine particulate matter  
45 at two San Jose Speciation Trends Network sites, *J. Air Waste Manage. Assoc.*, 56,  
46 1287-1300, 2006.
- 47 Kasumba, J., Hopke, P. K., Chalupa, D. C., and Utell, M. J.: Comparison of sources of  
48 submicron particle number concentrations measured at two sites in Rochester, NY, *Sci.*  
49 *total environ.*, 407, 5071-5084, 2009.



- 1 Kent, G. S., Yue, G. K., Farrukh, U. O., and Deepak, A.: Modeling atmospheric aerosol  
2 backscatter at CO<sub>2</sub> laser wavelengths. 1: Aerosol properties, modeling techniques, and  
3 associated problems, *Appl. Opt.*, 22, 1655-1665, 1983.
- 4 Kim, E., Hopke, P. K., Larson, T. V., and Covert, D. S.: Analysis of ambient particle size  
5 distributions using unmix and positive matrix factorization, *Environ. sci. tech.*, 38, 202-  
6 209, 2004.
- 7 Kim, E., and Hopke, P. K.: Source characterization of ambient fine particles in the Los  
8 Angeles basin, *J. Environ. Eng. Sci.*, 6, 343-353, 2007.
- 9 Kim, E., Turkiewicz, K., Zulawnick, S. A., and Magliano, K. L.: Sources of fine particles in  
10 the South Coast area, California, *Atmos. Environ.*, 44, 3095-3100, 2010.
- 11 Krecl, P., Hedberg Larsson, E., Ström, J., and Johansson, C.: Contribution of residential  
12 wood combustion and other sources to hourly winter aerosol in Northern Sweden  
13 determined by positive matrix factorization, *Atmos. Chem. Phys.*, 8, 3639-3653, 2008.
- 14 Li, N., Sioutas, C., Cho, A., Schmitz, D., Misra, C., Sempf, J., Wang, M., Oberley, T.,  
15 Froines, J., and Nel, A.: Ultrafine particulate pollutants induce oxidative stress and  
16 mitochondrial damage, *Environ/health perspect.*, 111, 455, 2003.
- 17 Lighty, J. S., Veranth, J. M., and Sarofim, A. F.: Combustion aerosols: factors governing  
18 their size and composition and implications to human health, *J. Air Waste Manage.*  
19 *Assoc.*, 50, 1565-1618, 2000.
- 20 Lim, H.-J., and Turpin, B. J.: Origins of primary and secondary organic aerosol in Atlanta:  
21 Results of time-resolved measurements during the Atlanta supersite experiment,  
22 *Environ. sci. tech.*, 36, 4489-4496, 2002.
- 23 Lim, J.-M., Lee, J.-H., Moon, J.-H., Chung, Y.-S., and Kim, K.-H.: Source apportionment of  
24 PM<sub>10</sub> at a small industrial area using Positive Matrix Factorization, *Atmos. Res.*, 95,  
25 88-100, 2010.
- 26 Lim, S. S., Vos, T., Flaxman, A. D., Danaei, G., Shibuya, K., Adair-Rohani, H., AlMazroa,  
27 M. A., Amann, M., Anderson, H. R., and Andrews, K. G.: A comparative risk  
28 assessment of burden of disease and injury attributable to 67 risk factors and risk factor  
29 clusters in 21 regions, 1990–2010: a systematic analysis for the Global Burden of  
30 Disease Study 2010, *Lancet*, 380, 2224-2260, 2013.
- 31 Liu, Z. R., Hu, B., Liu, Q., Sun, Y., and Wang, Y. S.: Source apportionment of urban fine  
32 particle number concentration during summertime in Beijing, *Atmos. Environ.*, 96, 359-  
33 369, 2014.
- 34 Miller, K. A., Siscovick, D. S., Sheppard, L., Shepherd, K., Sullivan, J. H., Anderson, G. L.,  
35 and Kaufman, J. D.: Long-term exposure to air pollution and incidence of  
36 cardiovascular events in women, *N. Engl. J. Med.*, 356, 447-458, 2007.
- 37 Moore, K. F., Ning, Z., Ntziachristos, L., Schauer, J. J., and Sioutas, C.: Daily variation in the  
38 properties of urban ultrafine aerosol—Part I: Physical characterization and volatility,  
39 *Atmos. Environ.*, 41, 8633-8646, 2007.
- 40 Na, K., Sawant, A. A., Song, C., and Cocker, D. R.: Primary and secondary carbonaceous  
41 species in the atmosphere of Western Riverside County, California, *Atmos. Environ.*,  
42 38, 1345-1355, 2004.
- 43 Nel, A., Xia, T., Mädlar, L., and Li, N.: Toxic potential of materials at the nanolevel, *Science*,  
44 311, 622-627, 2006.
- 45 Norris, G., Duvall, R., Brown, S., and Bai, S.: EPA Positive Matrix Factorization (PMF) 5.0  
46 Fundamentals and User Guide, U.S. Environmental Protection Agency, Office of  
47 Research and Development, Washington, DC 20460, 2014.
- 48 Oberdörster, G., Ferin, J., and Lehnert, B. E.: Correlation between particle size, in vivo  
49 particle persistence, and lung injury, *Environ. health perspect.*, 102, 173, 1994.



- 1 Oberdörster, G., Sharp, Z., Atudorei, V., Elder, A., Gelein, R., Lunts, A., Kreyling, W., and
- 2 Cox, C.: Extrapulmonary translocation of ultrafine carbon particles following whole-
- 3 body inhalation exposure of rats, *J. Toxicol. Environ. Health A*, 65, 1531-1543, 2002.
- 4 Ogulei, D., Hopke, P. K., and Wallace, L. A.: Analysis of indoor particle size distributions in
- 5 an occupied townhouse using positive matrix factorization, *Indoor Air*, 16, 204-215,
- 6 2006a.
- 7 Ogulei, D., Hopke, P. K., Zhou, L., Pancras, J. P., Nair, N., and Ondov, J. M.: Source
- 8 apportionment of Baltimore aerosol from combined size distribution and chemical
- 9 composition data, *Atmos. Environ.*, 40, 396-410, 2006b.
- 10 Ogulei, D., Hopke, P. K., Chalupa, D. C., and Utell, M. J.: Modeling source contributions to
- 11 submicron particle number concentrations measured in Rochester, New York, *Aerosol*
- 12 *Sci. Tech.*, 41, 179-201, 2007.
- 13 Paatero, P., and Tapper, U.: Analysis of different modes of factor analysis as least squares fit
- 14 problems, *Chemometr. Intell. Lab.*, 18, 183-194, 1993.
- 15 Paatero, P., and Tapper, U.: Positive matrix factorization: A non-negative factor model with
- 16 optimal utilization of error estimates of data values, *Environmetrics*, 5, 111-126, 1994.
- 17 Paatero, P.: Least squares formulation of robust non-negative factor analysis, *Chemometr.*
- 18 *Intell. Lab.*, 37, 23-35, 1997.
- 19 Paatero, P., Eberly, S., Brown, S. G., and Norris, G. A.: Methods for estimating uncertainty in
- 20 factor analytic solutions, *Atmos. Meas. Tech.*, 7, 781-797, 2014.
- 21 Peters, A., Wichmann, H. E., Tuch, T., Heinrich, J., and Heyder, J.: Respiratory effects are
- 22 associated with the number of ultrafine particles, *Am. j. respir. crit. care med.*, 155,
- 23 1376-1383, 1997.
- 24 Polidori, A., Arhami, M., Sioutas, C., Delfino, R. J., and Allen, R.: Indoor/outdoor
- 25 relationships, trends, and carbonaceous content of fine particulate matter in retirement
- 26 homes of the Los Angeles basin, *J. Air Waste Manage. Assoc.*, 57, 366-379, 2007.
- 27 Pope, C. A., Burnett, R. T., Thurston, G. D., Thun, M. J., Calle, E. E., Krewski, D., and
- 28 Godleski, J. J.: Cardiovascular mortality and long-term exposure to particulate air
- 29 pollution epidemiological evidence of general pathophysiological pathways of disease,
- 30 *Circulation*, 109, 71-77, 2004.
- 31 Pope Iii, C. A., Burnett, R. T., Thun, M. J., Calle, E. E., Krewski, D., Ito, K., and Thurston,
- 32 G. D.: Lung cancer, cardiopulmonary mortality, and long-term exposure to fine
- 33 particulate air pollution, *Jama*, 287, 1132-1141, 2002.
- 34 Reff, A., Eberly, S. I., and Bhave, P. V.: Receptor modeling of ambient particulate matter
- 35 data using positive matrix factorization: review of existing methods, *J. Air Waste*
- 36 *Manage Assoc.*, 57, 146-154, 2007.
- 37 Reid, J. S., Cahill, T. A., Wakabayashi, P. H., and Dunlap, M. R.: Geometric/aerodynamic
- 38 equivalent diameter ratios of ash aggregate aerosols collected in burning Kuwaiti well
- 39 fields, *Atmos. Environ.*, 28, 2227-2234, 1994.
- 40 Saffari, A., Hasheminassab, S., Shafer, M. M., Schauer, J. J., Chatila, T. A., and Sioutas, C.:  
41 Nighttime Formation of Aqueous-Phase Secondary Organic Aerosols in Los Angeles  
42 and its Implication for Fine Particulate Matter Composition and Oxidative Potential.,  
43 *Atmos. Environ.*, under review, 2016.
- 44 Schauer, J. J., and Cass, G. R.: Source apportionment of wintertime gas-phase and particle-
- 45 phase air pollutants using organic compounds as tracers, *Environ. sci. tech.*, 34, 1821-
- 46 1832, 2000.
- 47 Singh, M., Phuleria, H. C., Bowers, K., and Sioutas, C.: Seasonal and spatial trends in
- 48 particle number concentrations and size distributions at the children's health study sites
- 49 in Southern California, *J. Expo. Sci. Environ. Epidemiol.*, 16, 3-18, 2006.



- 1 Sioutas, C., Delfino, R. J., and Singh, M.: Exposure assessment for atmospheric ultrafine  
2 particles (UFPs) and implications in epidemiologic research, *Environ. health perspect.*,  
3 947-955, 2005.
- 4 Sofowote, U. M., Su, Y., Dabek-Zlotorzynska, E., Rastogi, A. K., Brook, J., and Hopke, P.  
5 K.: Sources and temporal variations of constrained PMF factors obtained from multiple-  
6 year receptor modeling of ambient PM 2.5 data from five speciation sites in Ontario,  
7 Canada, *Atmos. Environ.*, 108, 140-150, 2015.
- 8 Sowlat, M. H., Naddafi, K., Yunesian, M., Jackson, P. L., and Shahsavani, A.: Source  
9 apportionment of total suspended particulates in an arid area in southwestern Iran using  
10 positive matrix factorization, *B. environ. contam. tox.*, 88, 735-740, 2012.
- 11 Sowlat, M. H., Naddafi, K., Yunesian, M., Jackson, P. L., Lotfi, S., and Shahsavani, A.:  
12 PM10 source apportionment in Ahvaz, Iran, using positive matrix factorization,  
13 *CLEAN Soil Air Water*, 41, 1143-1151, 2013.
- 14 Stolzenburg, M., Kreisberg, N., and Hering, S.: Atmospheric size distributions measured by  
15 differential mobility optical particle size spectrometry, *Aerosol Sci. Tech.*, 29, 402-418,  
16 1998.
- 17 Strader, R., Lurmann, F., and Pandis, S. N.: Evaluation of secondary organic aerosol  
18 formation in winter, *Atmos. Environ.*, 33, 4849-4863, 1999.
- 19 Strawa, A. W., Elleman, R., Hallar, A. G., Covert, D., Ricci, K., Provencal, R., Owano, T.  
20 W., Jonsson, H. H., Schmid, B., and Luu, A. P.: Comparison of in situ aerosol  
21 extinction and scattering coefficient measurements made during the Aerosol Intensive  
22 Operating Period, *J. Geophys. Res. Atmos.* (1984–2012), 111, 2006.
- 23 Thimmaiah, D., Hovorka, J., and Hopke, P. K.: Source apportionment of winter submicron  
24 Prague aerosols from combined particle number size distribution and gaseous  
25 composition data, *Aerosol Air Qual Res*, 9, 209-236, 2009.
- 26 Venkatachari, P., Hopke, P. K., Grover, B. D., and Eatough, D. J.: Measurement of particle-  
27 bound reactive oxygen species in Rubidoux aerosols, *J Atmos Chem*, 50, 49-58, 2005.
- 28 Venkataraman, C.: Comparison of particle lung doses from the fine and coarse fractions of  
29 urban PM-10 aerosols, *Inhal toxicol*, 11, 151-169, 1999.
- 30 Vu, T. V., Delgado-Saborit, J. M., and Harrison, R. M.: Review: Particle number size  
31 distributions from seven major sources and implications for source apportionment  
32 studies, *Atmos Environ*, 122, 114-132, 2015.
- 33 Watson, J. G., Chow, J. C., Lowenthal, D. H., Stolzenburg, M. R., Kreisberg, N. M., and  
34 Hering, S. V.: Particle size relationships at the Fresno supersite, *J Air Waste Manage*  
35 *Assoc.*, 52, 822-827, 2002.
- 36 Wichmann, H.-E., Spix, C., Tuch, T., Wölke, G., Peters, A., Heinrich, J., Kreyling, W. G.,  
37 and Heyder, J.: Daily mortality and fine and ultrafine particles in Erfurt, Germany part  
38 I: role of particle number and particle mass, Research report (Health Effects Institute),  
39 5-86, 2000.
- 40 Yue, W., Stölzel, M., Cyrus, J., Pitz, M., Heinrich, J., Kreyling, W. G., Wichmann, H. E.,  
41 Peters, A., Wang, S., and Hopke, P. K.: Source apportionment of ambient fine particle  
42 size distribution using positive matrix factorization in Erfurt, Germany, *Sci. total*  
43 *environ.*, 398, 133-144, 2008.
- 44 Zhang, K. M., Wexler, A. S., Niemeier, D. A., Zhu, Y. F., Hinds, W. C., and Sioutas, C.:  
45 Evolution of particle number distribution near roadways. Part III: Traffic analysis and  
46 on-road size resolved particulate emission factors, *Atmos. Environ.*, 39, 4155-4166,  
47 2005.
- 48 Zhou, L., Hopke, P. K., Stanier, C. O., Pandis, S. N., Ondov, J. M., and Pancras, J. P.:  
49 Investigation of the relationship between chemical composition and size distribution of



1 airborne particles by partial least squares and positive matrix factorization, J. Geophys.  
2 Res. Atmos., (1984–2012), 110, 2005.  
3 Zhou, L., Kim, E., Hopke, P. K., Stanier, C. O., and Pandis, S.: Advanced factor analysis on  
4 Pittsburgh particle size-distribution data special issue of aerosol science and technology  
5 on findings from the Fine Particulate Matter Supersites Program, Aerosol Sci. Tech.,  
6 38, 118-132, 2004.  
7  
8  
9  
10  
11  
12  
13  
14  
15  
16  
17  
18  
19  
20  
21  
22  
23  
24  
25  
26  
27  
28  
29  
30  
31  
32  
33  
34  
35  
36



1 Table 1. Summary of the input parameters to the PMF model in this study.

Parameter	Source of data	Time resolution in original data set
EC, OC	Sunset monitor	1 hr
Size Distribution (14-760 nm)	SMPS	5 min
Size Distribution (0.3-10 $\mu\text{m}$ )	OPS	5 min
BC	Aethalometer	15 min
PM mass concentration data ( $\text{PM}_{10-2.5}$ , $\text{PM}_{2.5}$ )	CARB	1 hr
Gaseous Pollutants ( $\text{NO}$ , $\text{NO}_2$ , $\text{CO}$ , $\text{O}_3$ , $\text{SO}_2$ )	CARB	1 hr
Meteorological data (T, RH, WS)	CARB	1 hr
Traffic data (counts of LDV and HDV)	PeMS	1 hr

2  
3  
4  
5  
6  
7  
8  
9  
10  
11  
12  
13  
14  
15  
16  
17  
18  
19  
20  
21  
22  
23  
24  
25  
26



1

2 Table 2. Summary statistics for the parameters included in the PMF model.

Species	Geometric Mean	Standard Error	Min	Max	S/N ratio
Total number concentration ( $\#/cm^3$ )	6860.00	94.10	524.00	32400.00	7.00
PM <sub>10-2.5</sub> ( $\mu g/m^3$ )	15.90	0.19	2.00	77.00	7.00
PM <sub>2.5</sub> ( $\mu g/m^3$ )	14.50	0.23	1.00	101.00	6.90
CO (ppm)	0.58	0.01	0.10	2.19	7.10
NO (ppb)	8.46	0.57	1.00	212.00	5.80
NO <sub>2</sub> (ppb)	22.50	0.23	1.90	75.00	7.10
O <sub>3</sub> (ppb)	17.40	0.33	2.00	105.00	6.80
BC ( $\mu g/m^3$ )	1.14	0.02	0.124	9.13	6.90
POC* ( $\mu g/m^3$ )	2.20	0.08	0.10	19.20	6.80
SOC* ( $\mu g/m^3$ )	2.13	0.05	0.04	16.30	7.10
EC* ( $\mu g/m^3$ )	1.01	0.03	0.01	7.34	8.80
RH (%)	50.40	0.40	6.00	99.00	7.10
Temperature ( $^{\circ}C$ )	18.80	0.13	3.89	38.33	7.30
Wind speed (m/s)	4.03	0.04	1.00	14.00	6.80
LDV (#/h)	3790	34	691	7620	7.10
HDV (#/h)	153	3	5	920	6.80

3

\*Values are pertaining to the runs including EC/OC data.

4

5

6

7

8

9

10

11

12

13

14

15

16

17

18

19

20

21

22

23

24

25



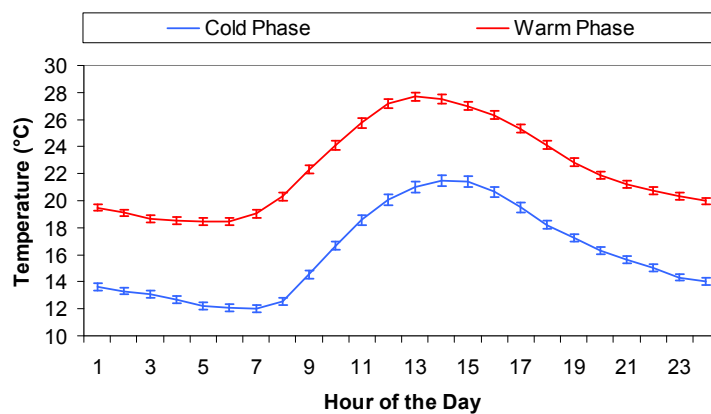
1 Table 3. Spearman correlation coefficient matrix indicating the association between the  
 2 auxiliary variables and the factors resolved by the PMF model. R values above 0.5 are  
 3 bolded.  
 4

Species	Nucleation	Traffic 1	Traffic 2	Urban Background Aerosol	Secondary Aerosol	Soil/Road Dust
PM <sub>10-2.5</sub>	0.17*	0.21*	0.35*	0.27*	0.09*	0.39*
PM <sub>2.5</sub>	-0.24*	-0.09*	0.05*	0.33*	<b>0.69*</b>	0.23*
CO	0.04	0.41*	<b>0.58*</b>	<b>0.64*</b>	0.17*	0.28*
NO	-0.01	0.48*	<b>0.59*</b>	<b>0.52*</b>	0.27*	0.24*
NO <sub>2</sub>	0.08*	<b>0.50*</b>	<b>0.60*</b>	<b>0.57*</b>	0.33*	0.14*
O <sub>3</sub>	<b>0.57*</b>	0.34*	0.40*	-0.35*	0.46*	0.19*
BC	0.01	<b>0.53*</b>	<b>0.70*</b>	<b>0.71*</b>	0.13*	0.22*
POC	0.09*	<b>0.62*</b>	0.28*	0.30*	0.24*	0.29*
SOC	0.46*	0.12*	0.43*	<b>0.58*</b>	0.46*	0.20*
EC	0.17*	0.47*	<b>0.56*</b>	<b>0.60*</b>	0.20*	0.17*
RH	-0.26*	-0.32*	-0.30*	-0.05*	0.43*	0.33*
Temp	<b>0.52*</b>	-0.23*	-0.18*	-0.39*	0.34*	0.47*
WS	<b>0.57*</b>	0.00	0.07*	-0.04*	-0.25*	<b>0.62*</b>
LDV	0.22*	<b>0.70*</b>	0.42*	0.05*	0.01	0.02
HDV	0.23*	<b>0.52</b>	0.43*	-0.08*	-0.12*	-0.01

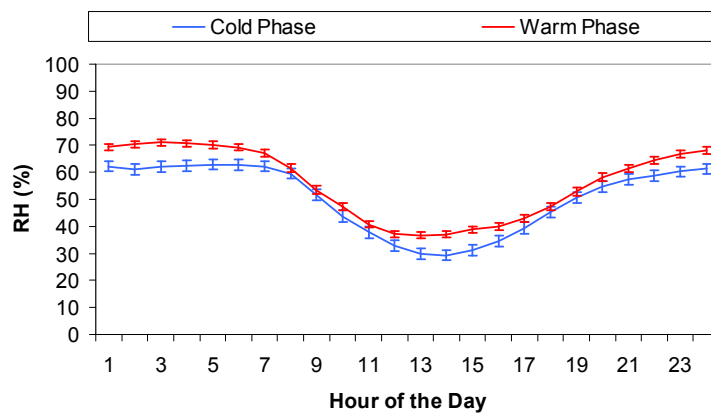
5 \* Indicates R values that are statistically significant (P<0.05).  
 6  
 7  
 8  
 9  
 10  
 11  
 12  
 13  
 14  
 15  
 16  
 17  
 18  
 19  
 20  
 21  
 22  
 23  
 24  
 25  
 26  
 27  
 28  
 29  
 30  
 31  
 32  
 33



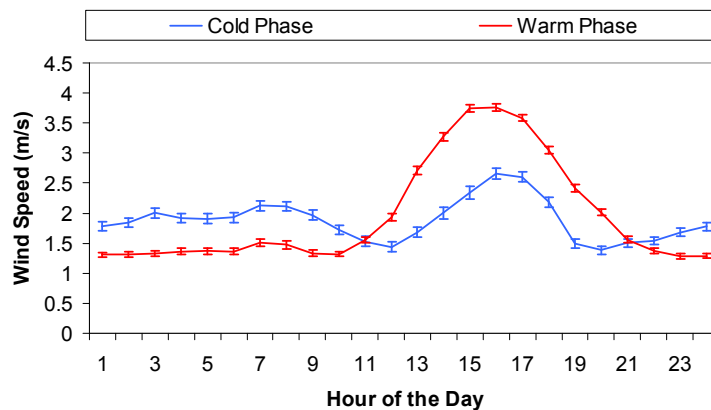
- 1 Figure 1. Diurnal variations of important meteorological parameters in the cold and warm
- 2 phases. Error bars correspond to one standard error.



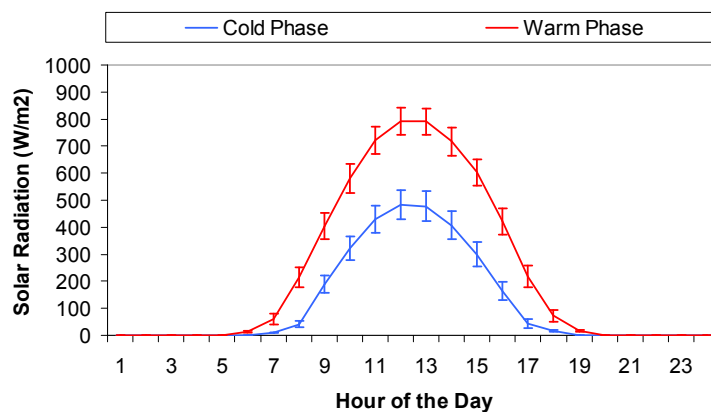
3



4



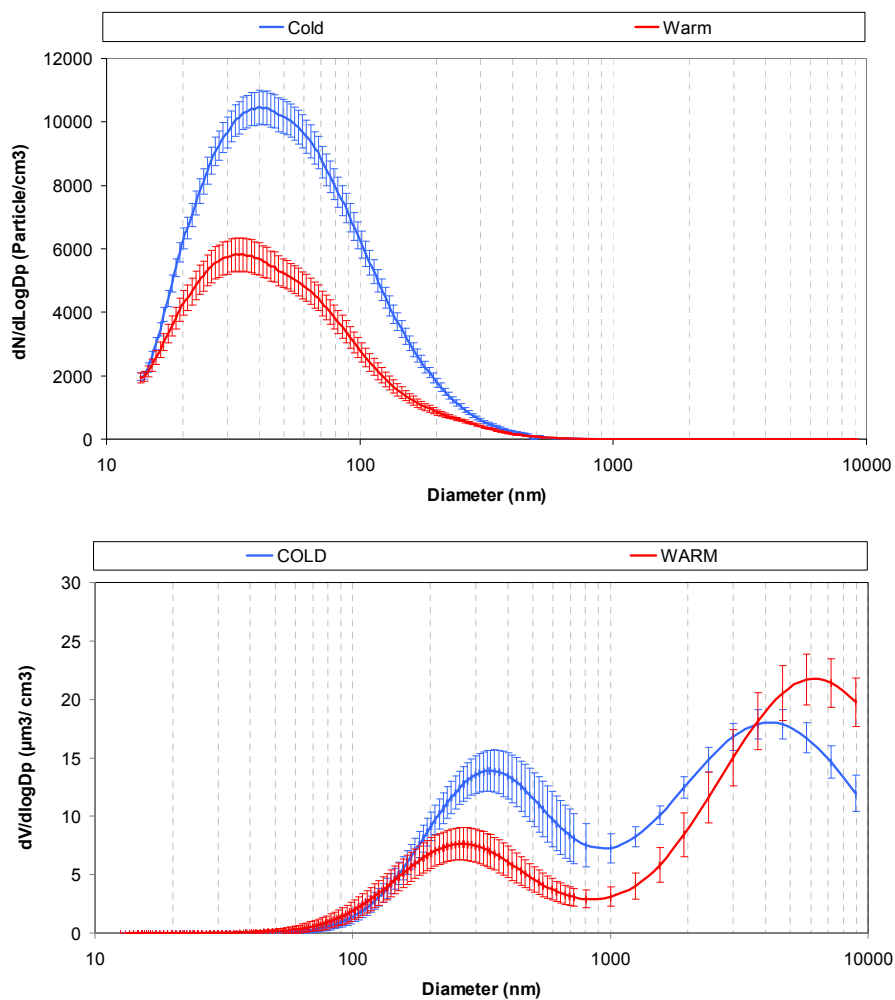
5



1  
2  
3  
4  
5  
6  
7  
8  
9  
10  
11  
12  
13  
14  
15  
16  
17  
18  
19  
20  
21  
22  
23  
24  
25  
26  
27  
28  
29  
30  
31  
32  
33  
34  
35  
36



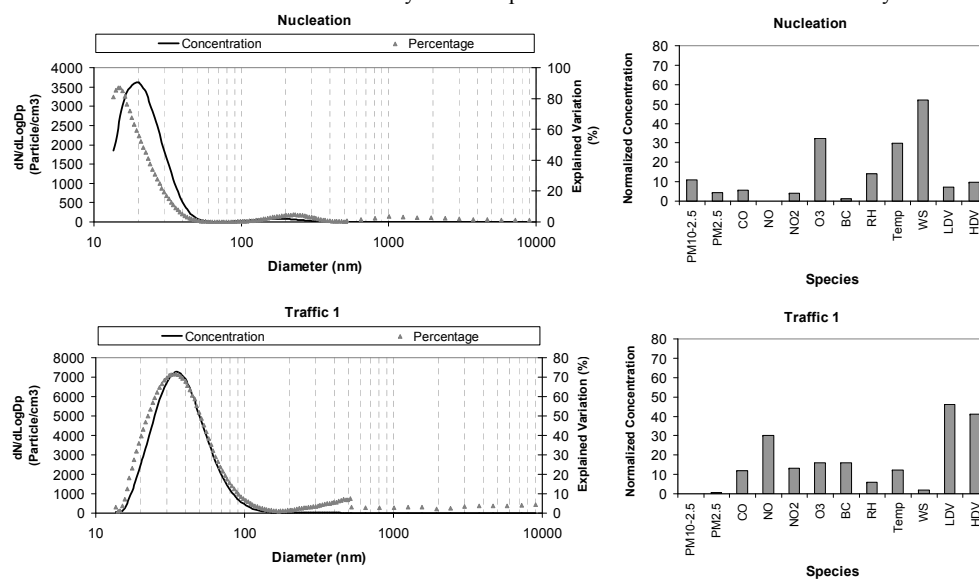
1 Figure 2. Average number and volume size distributions of all the input samples to the PMF  
2 model in the cold and warm phases (the graphs represent geometric means  $\pm$  SE).



3  
4  
5  
6  
7  
8  
9  
10  
11  
12  
13  
14  
15  
16

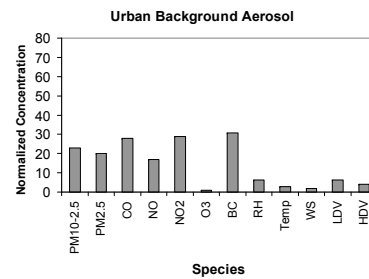
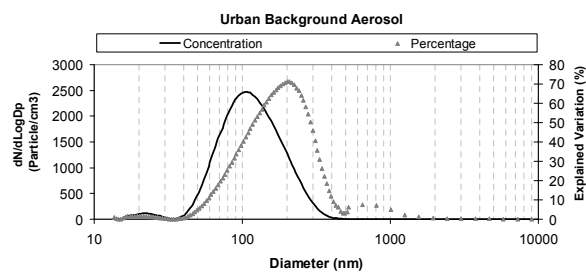
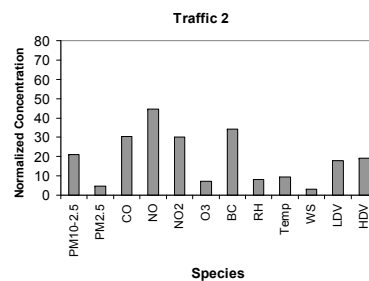
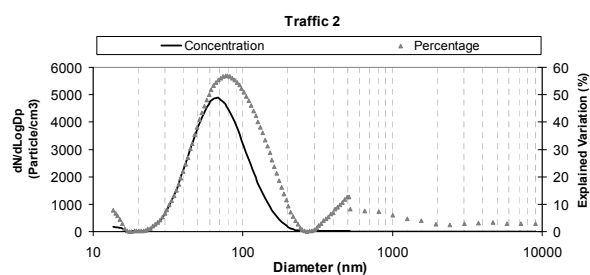


1 Figure 3. The number size distributions as well as the auxiliary variables profiles for each of the factors resolved by the PMF model.



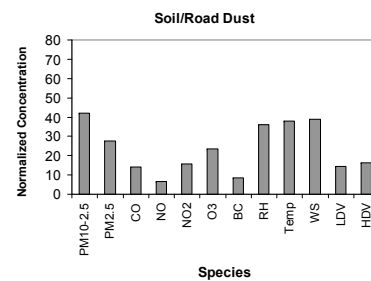
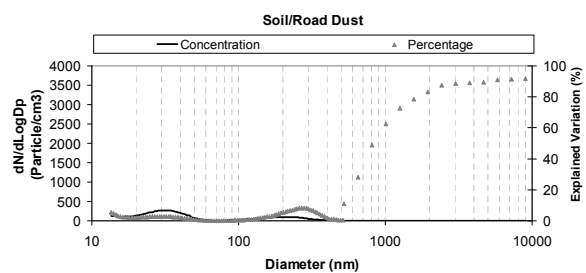
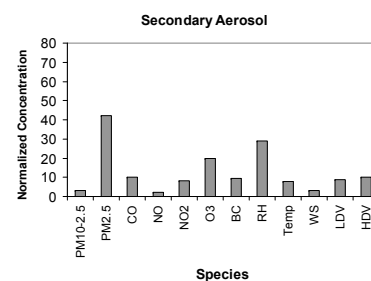
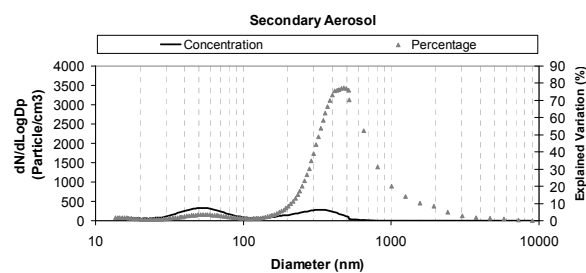
2

3



1

2

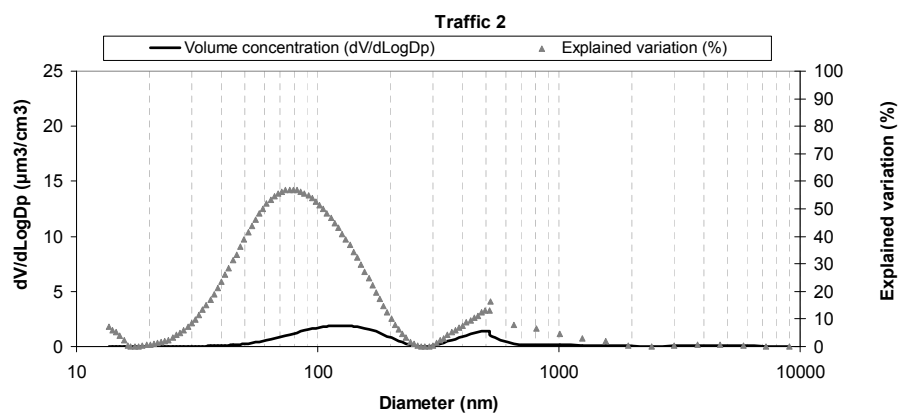
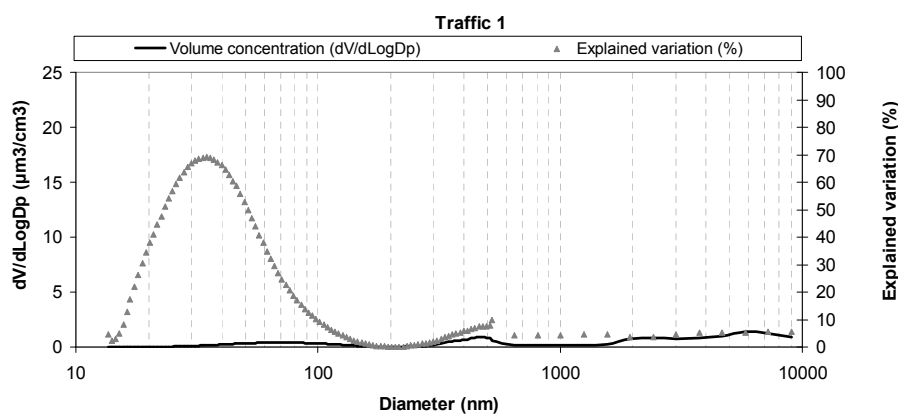
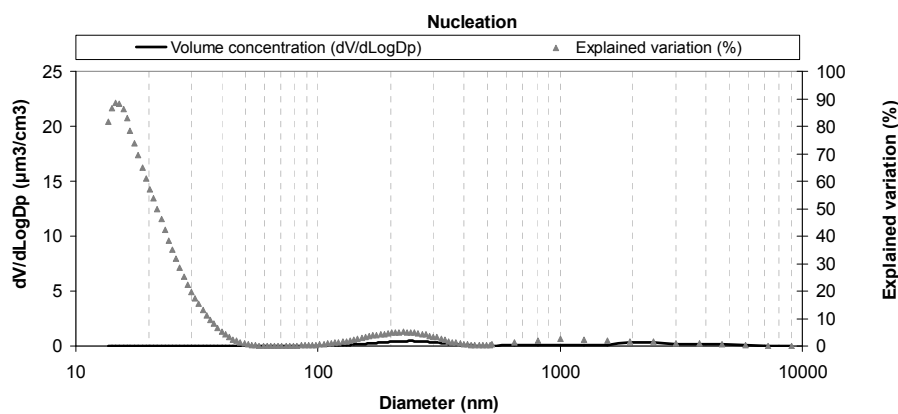


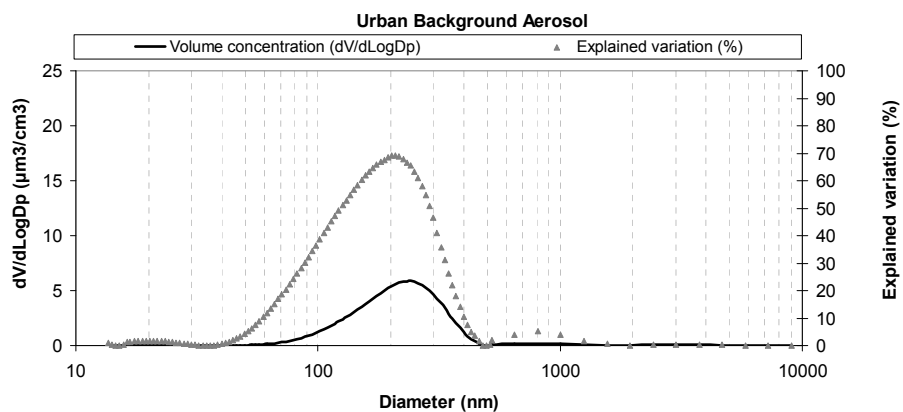
1

2  
3  
4  
5  
6  
7  
8  
9  
10  
11  
12

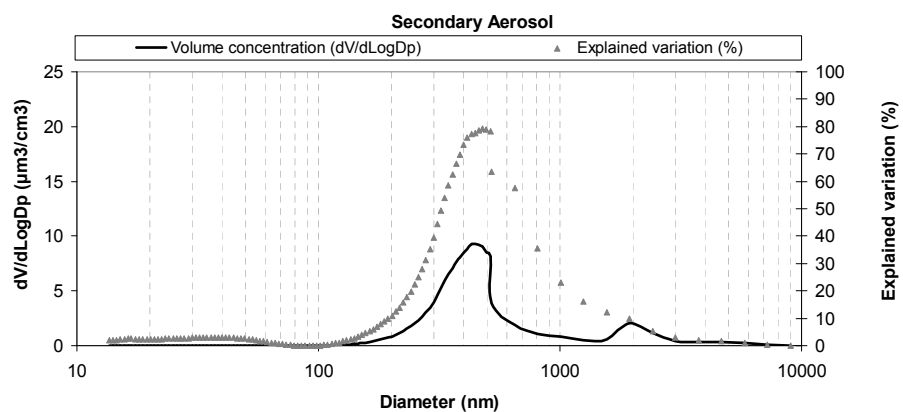


- 1 Figure 4. Volume size distributions along with the explained variation (%) of each factor
- 2 profile resolved by the PMF model.

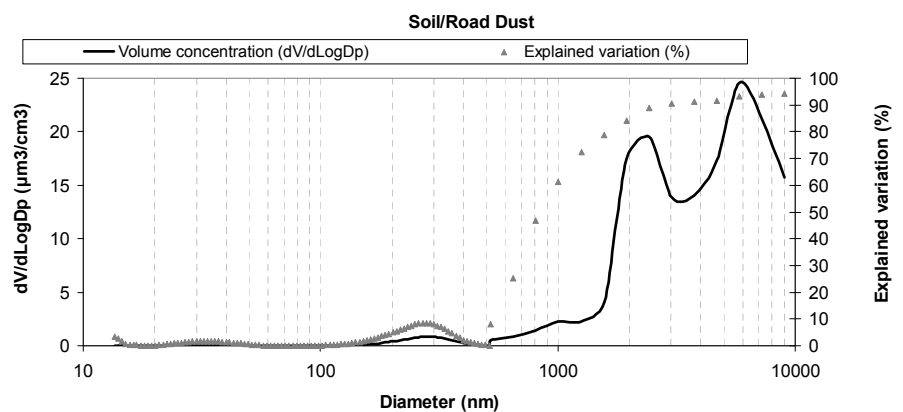




1



2



3

4

5

6

7

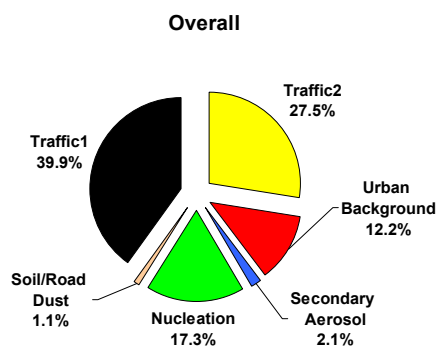
8

9

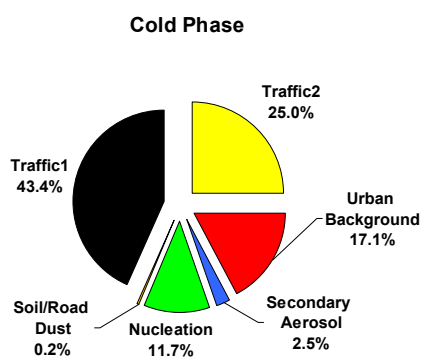


- 1 Figure 5. Relative contribution of each factor to the total number concentrations: a) overall
- 2 phases; b) cold phase; and c) warm phase.

3



4



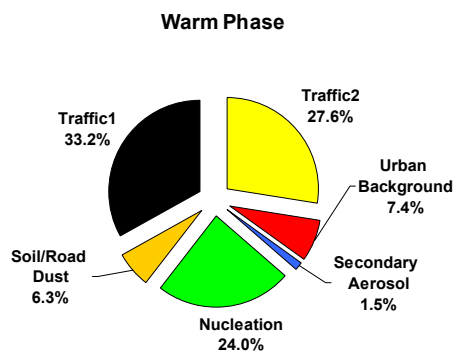
5

6

7

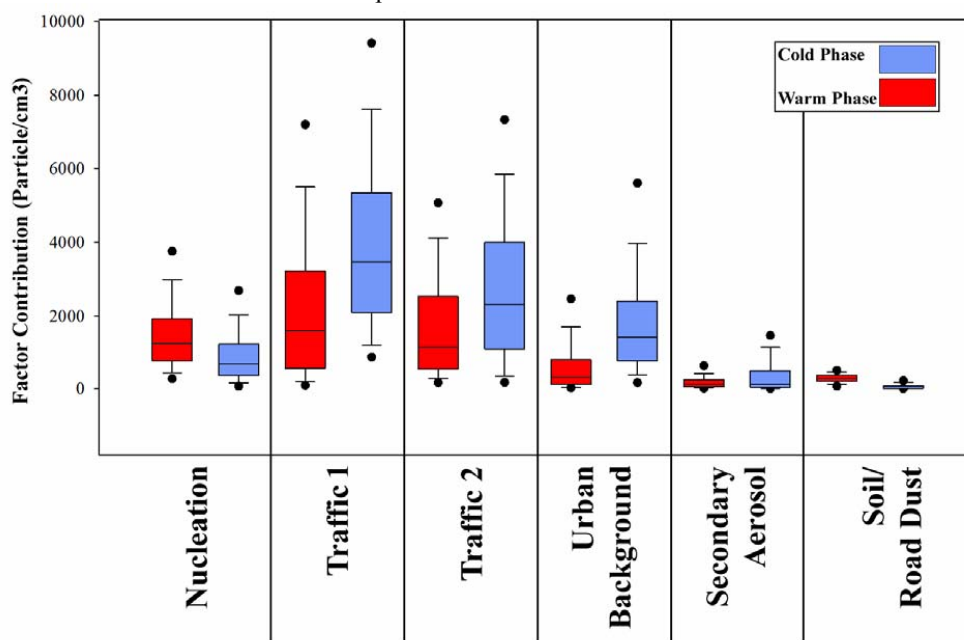
8

9





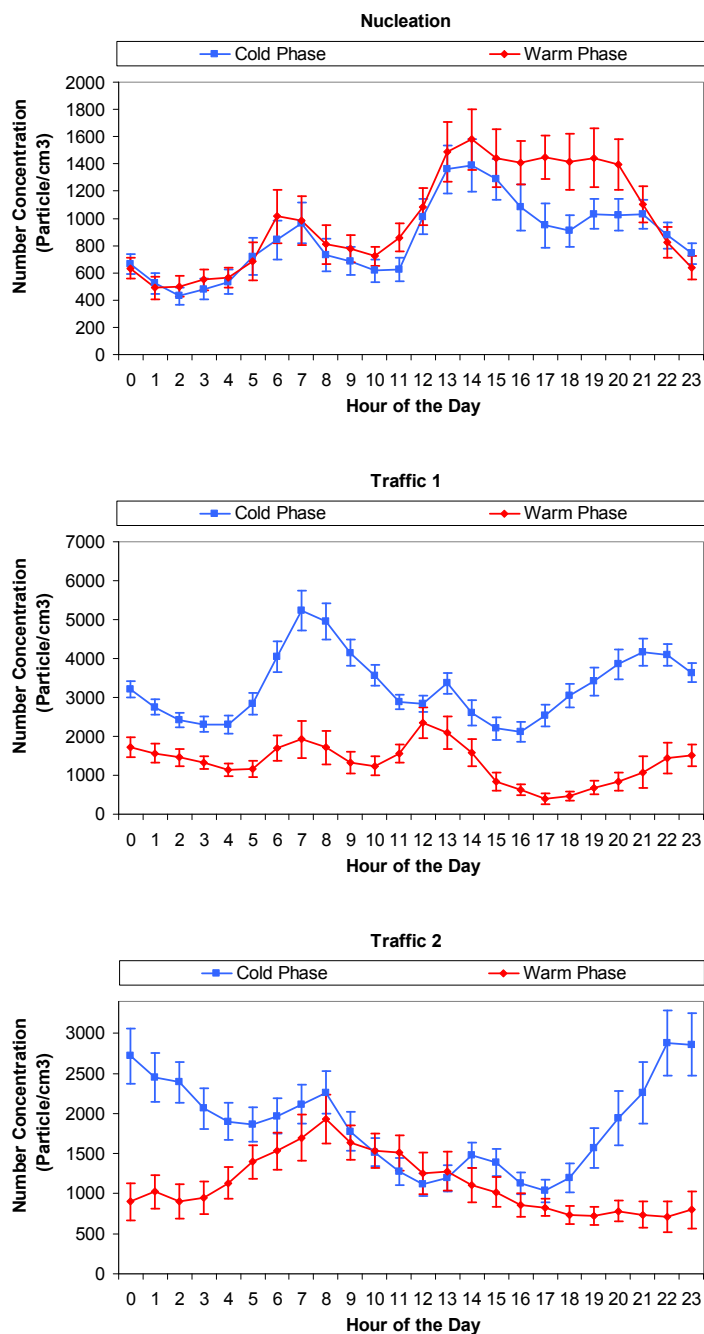
1 Figure 6. Contribution (particles/cm<sup>3</sup>) of each of the PMF-resolved factors to the total number  
2 concentrations in the cold and warm phases.



3  
4  
5  
6  
7  
8  
9  
10  
11  
12  
13  
14  
15  
16  
17  
18  
19  
20  
21  
22  
23  
24  
25  
26  
27  
28  
29



- 1 Figure 7. Diurnal variations (geometric means) of number concentrations (particles /cm<sup>3</sup>)
- 2 from each factor resolved by the PMF model in the cold and warm phases. Error bars
- 3 correspond to one standard error.



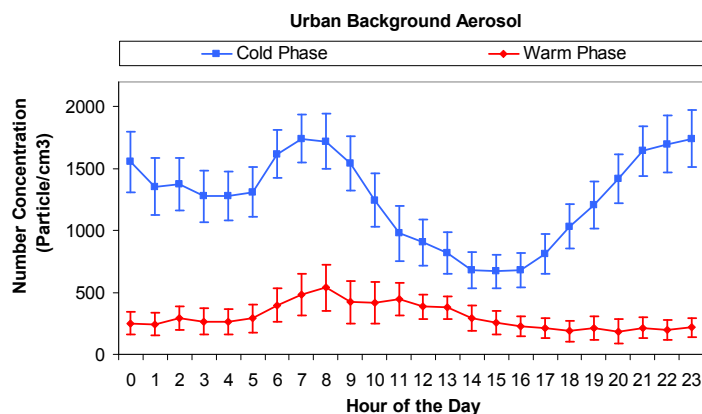
4  
5

6  
7

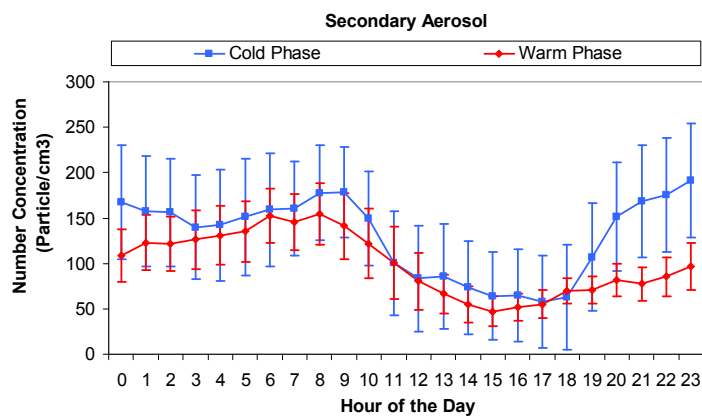
8



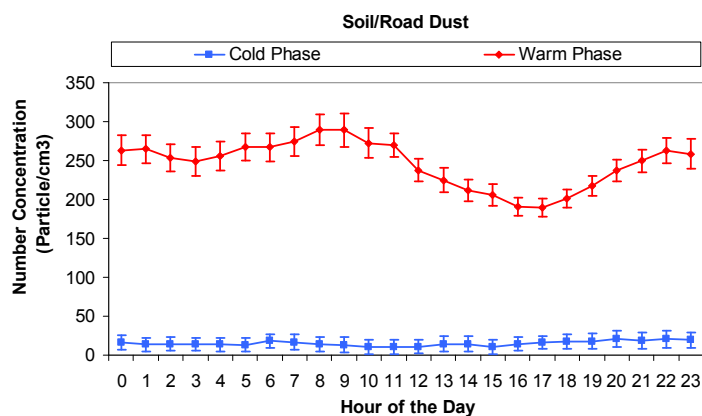
1



2

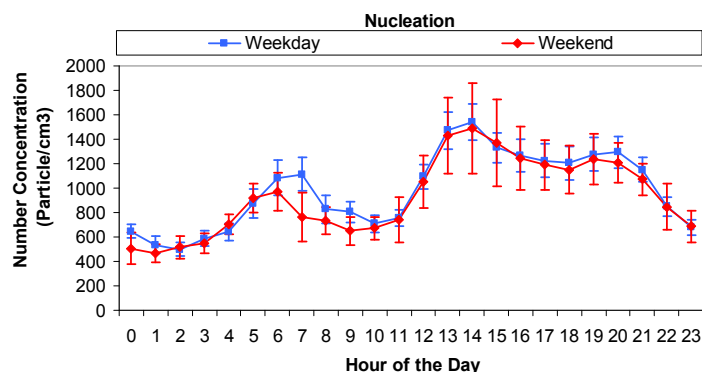


3  
4  
5  
6  
7  
8  
9  
10

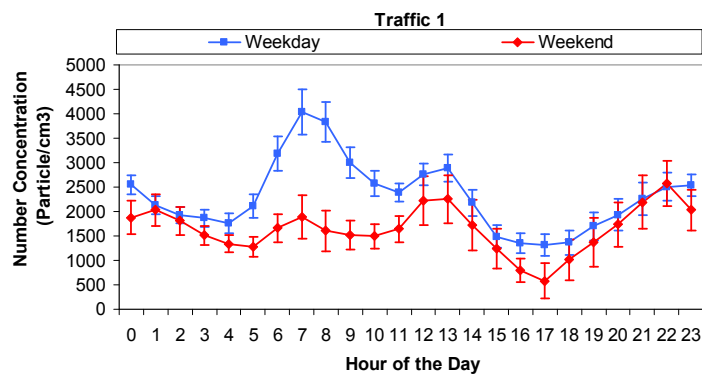




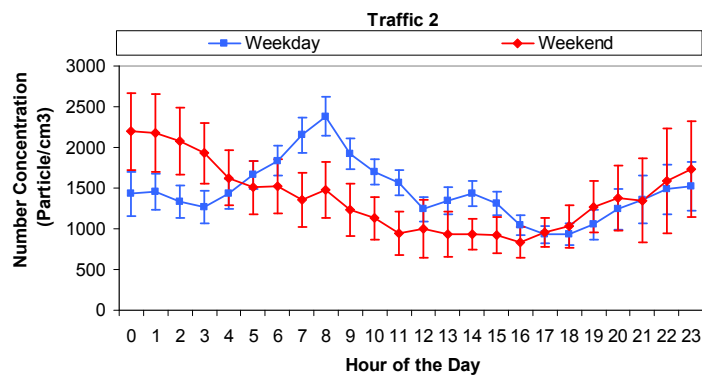
- 1 Figure 8. Weekday/weekend analysis of each of the factors resolved by the PMF model
- 2 (values are geometric means). Error bars correspond to one standard error.



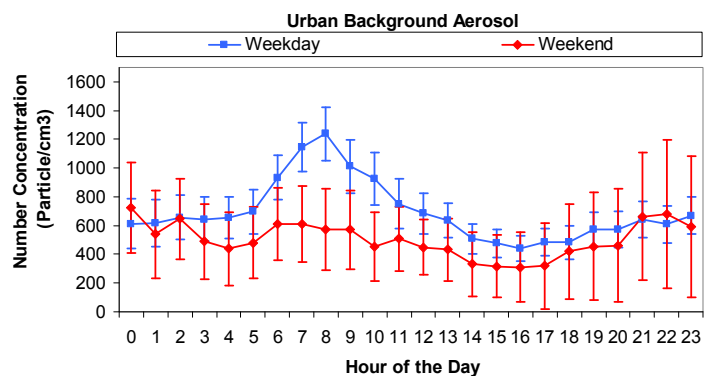
3



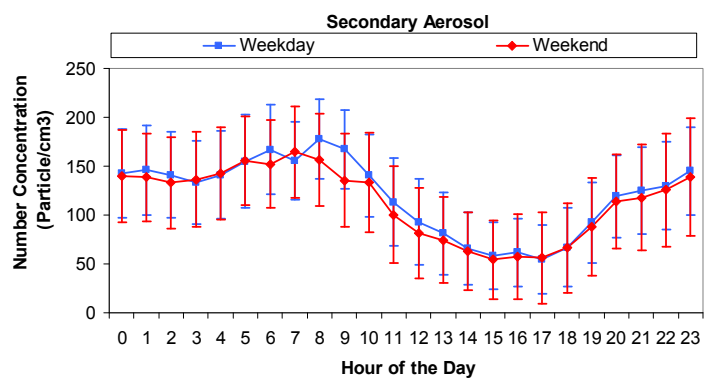
4



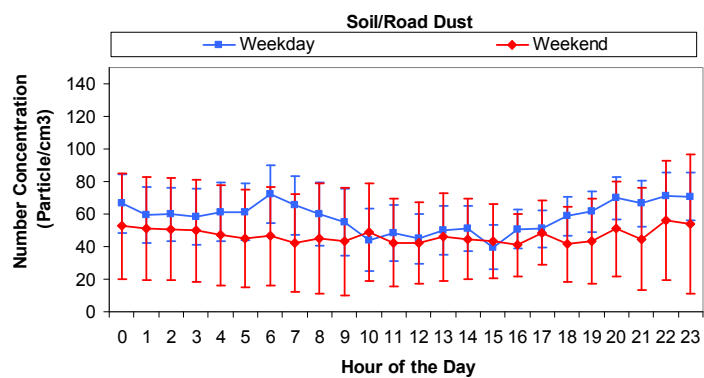
5



1



2



3  
4  
5  
6  
7  
8  
9  
10  
11  
12  
13  
14